Clean Technologies and Environmental Policy (2026) 28:70
https://doi.org/10.1007/s10098-025-03379-3

ORIGINAL PAPER

Harnessing the bio-structure of corncobs: connecting morphology to mechanical attributes for sustainable building materials

Francis O. Okeke[1] · Abdullahi Ahmed[1,2] · Adil Imam[1] · Hany Hassanin[1]

Received: 24 June 2025 / Accepted: 13 October 2025 / Published online: 2 February 2026

Abstract

The escalating global emphasis on sustainable construction and renewable materials has highlighted agricultural waste valorization as a critical research domain, particularly in response to the climate emergency. As the construction industry seeks alternative ecofriendly materials to mitigate environmental impact and expand affordable housing solutions, there is a pressing need to explore and evaluate suitable biomass resources in greater depth. Among these, corncob (CC) emerges as a significantly underutilized material with considerable potential for sustainable applications. Despite its abundance and promising properties, systematic understanding of the composition–structure–function relationships within CC anatomical fractions remains limited, impeding its optimal utilization in building and construction. This study employs a multi-analytical approach to investigate the intricate correlations between CC morphology, mechanical attributes, and chemical composition to establish its viability as a sustainable building material (SBM). The methodology integrated microscopic analysis (SEM–EDS), mechanical characterization, and chemical assays. Microscopy reveals differentiated ultrastructure that collectively confer balanced strength–ductility attributes. Elemental mapping demonstrated predominant carbon (64.73–67.74%) and oxygen (31.22–34.05%) composition, with strategic distributions of silicon (2.52%) and aluminum (0.69%) contributing to mechanical properties. Mechanical testing showed compressive strength (67.6 MPa) attributable to the lignocellulosic reinforcement grid resisting fractures. Comparatively, tensile testing indicates elasticity (Young's modulus 191.19 MPa), exceeding most agricultural residues resulting from interfibrillar sliding mechanisms accommodating strains. Chemical analysis revealed optimal lignocellulosic composition complemented by functional additives (1% pectin, 4.21% resistant starch). Integrated morphological and mechanical characterization coupled with compositional mapping and the preliminary life cycle assessment substantiate cob waste as an economical bio-based substitute for mainstream building insulation, 3D printing, carbon sequestering, structural, and non-structural applications. The multi-level examination provides understanding of structure–function influences to direct processing interventions for customized material properties.

✉ Francis O. Okeke
f.okeke142@canterbury.ac.uk

[1] School of Engineering, Technology and Design, Canterbury Christ Church University, Canterbury, Kent, UK CT1 1QU

[2] School of Architecture, Built Environment, Computing and Engineering, Birmingham City University, B4 7BD Birmingham, UK

Graphical abstract

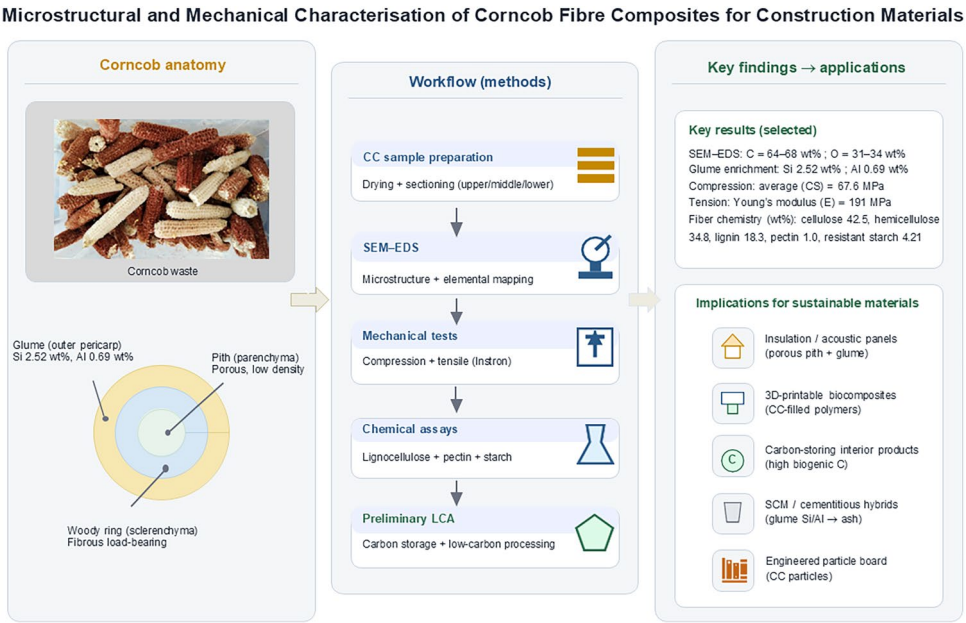

Keywords Biomass · Building construction · Corncob · Mechanical · Sustainable material

Introduction

Despite ongoing efforts to decrease energy usage and promote the incorporation of sustainable materials in buildings, the building and construction sector continues to account for a substantial portion of global energy and resources consumption (Mayernik 2020). With a continuously expanding global population, there is an escalating urgency to utilize natural resources sustainably to mitigate environmental strains (Okeke et al. 2020). Studies project that intensified agricultural processing will produce unprecedented quantities of food by-products and waste (Kummu et al. 2012). In light of contemporary societal priorities, healthier and ecologically conscious lifestyles have entered mainstream consciousness, reflected through reduced consumer waste and improved food utilization (Aschemann-Witzel et al. 2015; de Hooge et al. 2017). Recent surveys indicate environmental impact now represents one of the foremost considerations influencing food selection across international markets (Grunert et al. 2014). This universal paradigm shift emphasizes prudent management of food by-products and waste as instrumental in upholding population needs without compromising future resource availability or ecological stability (Gustavsson et al. 2011). The growing waste crisis worldwide has led to immense interest in repurposing agricultural industry residues into value-added sustainable materials.

Corn (Zea mays L.) is a staple cereal crop cultivated annually, with the United States being the largest single producer (U.S., 2025). Corn waste in the US accounts for one-third of the total generated solid waste (U.S. Environmental Protection Agency 2021; Penn 2006). According to the Food and Agriculture Organization (FAO 2023), approximately 1.23 billion metric tons were harvested in 2022–23, worth $284.16 billion. Specifically, CC is a waste residue produced after corn harvesting and grain removal, which represents about 14% of grain yield corresponding to approximately 16% of total corn stover in a field (Castorina et al. 2023). According to Wojcieszak et al. (2022), CC account for over 20% of total aboveground residues based on dry weight. On a global scale, this equates to roughly 164 teragrams (Tg) of CCs generated annually (Takada et al. 2018). In many developing economies, these cobs are frequently discarded or relegated to low-value uses such as animal feed, while in developed settings substantial volumes of these lignocellulosic residues are recycled as soil amendments or low-grade fuel (Yanni et al. 2013) and their utilization as sustainable biomaterials for diverse industrial applications like packaging or textiles is receiving increasing attention (Sun et al. 2004). However, CC contains high fibrous material that has the potential to be utilized as a sustainable construction material. As one of the highest produced cereal crops globally (see Fig. 1), corn cultivation yields

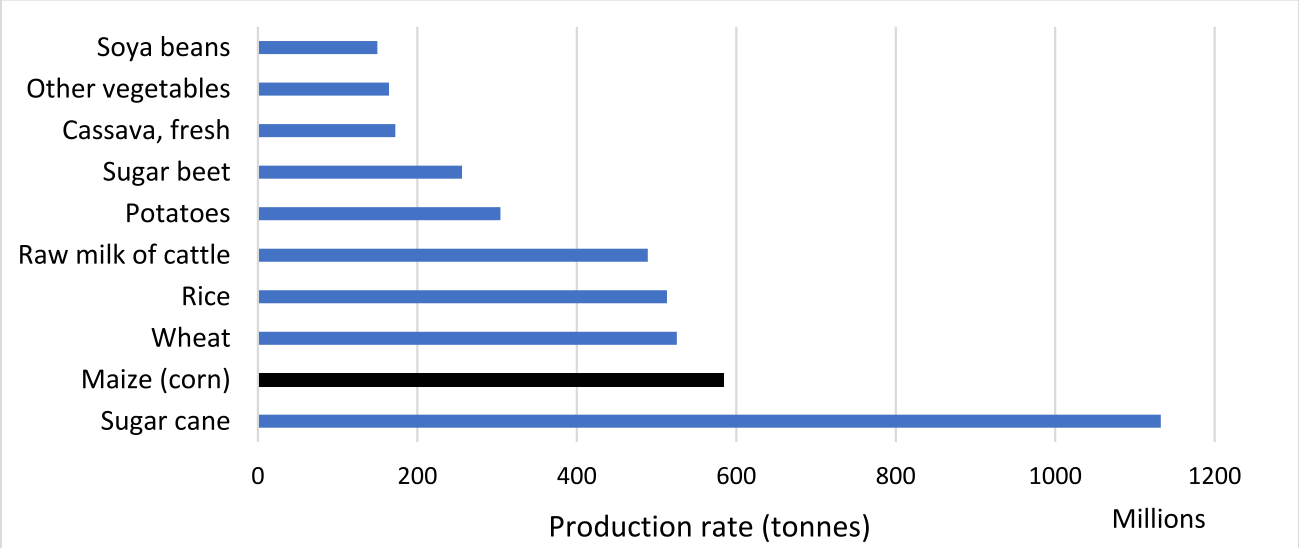

Fig. 1 Worldwide most produced food commodity from 1961 to 2022 *Source* FAO, (2023)

substantial CC waste that contains natural fiber (Reddy and Yang 2005a). The intricate fibrillar anatomy in plant biomass confers advantageous mechanical properties related to factors like cell wall thickness, microfibril angle, and chemical composition (Kabir et al. 2013).

Recently, lignocellulosic fibers have been shown to serve effectively as sustainable reinforcement elements or binders in composite bricks, insulation boards, wall panels, and decking materials (Andrew & Dhakal 2022). Research on novel plant fibers further reinforces the importance of systematically linking fiber morphology to composite performance. For example, Napier grass fiber incorporated into a PLA matrix with porcelain particulates delivered notable mechanical improvements, with SEM analysis confirming strong fiber–matrix interfacial bonding facilitated by the porcelain "bridging" effect (Thandavamoorthy & Devarajan 2024). Similarly, fibers extracted from *Coccinia grandis* have been comprehensively characterized, revealing cellulose Iβ structure, a crystallinity index of 46%, tensile strength of 775 MPa, and Young's modulus values that affirm their suitability as reinforcement in polymer composites (Jebadurai et al. 2019). In parallel, henequen (*Agave fourcroydes*) leaf fibers have been validated as effective reinforcements in polypropylene (PP) composites, where coupling agents enhanced fiber–matrix adhesion and positioned henequen as a credible bio-based alternative to sized glass fiber in selected applications (Espinach et al. 2022; Serra-Parareda et al. 2021). Collectively, these studies illustrate a broader research trend: When fiber ultrastructure and chemistry are systematically characterized and aligned with processing methods, natural fibers can achieve meaningful stiffness and strength at low density while also providing thermal and acoustic benefits. Nevertheless, the applicability of the above studied natural fibers is often constrained by regional availability and limitations in versatility for global adoption.

CC have also demonstrated potential, particularly as fillers in wood–plastic composites and bio-adhesives (Goel 2021), yet systematic investigations linking their multiscale morphology to mechanical performance remain scarce. Reddy & Yang (2005b) examined cornstalk fibers, noting their potential for textile processing and blending with other fibers, while Okeke et al. (2024b) explored CC ash for its suitability in building applications. Numerical simulations by Tao & Wei (2020) and Yan (2017) have modeled the mechanical attributes and impact dynamics of CC structures at a macroscopic scale. However, such studies did not account for microstructural variations across cob tissues. Understanding these variations is critical, as they govern strength, rigidity, absorption, and processability; factors central to targeted applications in construction. A limited number of studies have touched on processing methods and composite fabrication with CC fibers (Sagar et al. 2018), and Yu (2014) experimentally measured bulk mechanical parameters through compression, shear, and bending tests. However, most of the existing literature has treated CC biomass as a homogeneous material. Okeke et al. (2024a) provided a comprehensive review cataloging potential applications but did not generate new insights into structure–property relationships. Zou et al. (2021) investigated microstructural effects on compression behavior, though without fully exploring anatomical stratification and multifunctional performance. Pinto et al. (2012) characterized CC microstructure and composition, demonstrating its use in traditional *tabique* construction in Portugal, but did not

extend analysis to reinforcement in advanced composites or load-bearing applications. Their study also lacked compositional analyses needed to correlate fibrous content with mechanical behavior.

From the foregoing, while prior research has established foundational knowledge of CC properties and potential uses, there remains a significant gap in correlating the intricate, tissue-specific microarchitecture of CCs with their mechanical performance. Addressing this gap is the central aim of the present study. Specifically, this work investigates the anatomical structure, elemental composition, and fibrous content of CC and evaluates their relationship to tensile and compressive properties. The study objectives are threefold: (i) microscopic visualization via SEM coupled with elemental analysis using energy-dispersive X-ray spectroscopy (EDS) to characterize cob structure; (ii) quantification of key mechanical forces related to crushing and tension using standardized universal testing protocols; and (iii) assessment of fiber and starch fractions to interpret their influence on mechanical properties. By bridging micro- and macro-scale insights, this study advances understanding of how structural heterogeneity governs CC performance. The novelty lies in linking microstructural heterogeneity of CC to functional performance metrics, thereby offering insights that can guide tailored valorization of CCs as plant-based reinforcements in sustainable construction materials. In doing so, this study contributes not only to reducing agricultural waste but also to expanding the palette of renewable, locally available resources for the building industry.

Cradle-to-grave development and use of corn

The corn life cycle consists of distinct vegetative and reproductive phases culminating in grain production and senescence. Germination initiates with the coleoptile and radical emerging from seed, followed by successive leaf stages facilitating rapid early season expansion through optimal solar capture and photosynthetic output (Nafziger 2003). The onset of reproductive stages commences with male tassels releasing pollen for wind dispersal to female silks, enabling double fertilization events that precipitate kernel initiation atop successfully pollinated ovaries within corn ears (Uribelarrea et al. 2004). Ensuing phases foster dynamic biochemical exchanges between developing ears and the remaining plant, facilitating nutrient import supporting embryo maturation and grain fill (Setter et al. 2001). Final maturation dries and hardens kernels in preparation for harvesting ears as primary yield components.

The primary end-product of corn agriculture is the grain itself, while residual biomass comprising stalks, husks, leaves, and cobs represents around half the total yield but is regarded as waste after grain harvest (Kim & Dale 2004). Traditionally, most corn stover resources were left discarded on agricultural fields post-reaping or set ablaze in open air, as inadequate market channels diminish prospects for by-product utilization (Gallagher et al. 2003). However, with escalating environmental pressures, nascent bio-based industries now recognize agricultural waste as a valuable yet overlooked bioresource with untapped potential (Brassard et al. 2016). Adopting an integrative approach reconciling commercial viability with ecological stability represents the critical next step in maximizing the conversion efficiency of each corn harvest. Among corn residues, the CC specifically demonstrates unique traits conferring utility across bio-industries. Extensive analyses verify agricultural and ecological impacts from on-field cob decomposition remain negligible (Blanco-Canqui & Lal 2007; Johnson et al. 2006). CCs offer only modest surface cover against erosion and runoff, return relatively little nutrients through slow decay, and their soluble constituents are readily leached by rainfall, diminishing any fertilization effect (Bonin & Lal 2012). In view of this balance of properties, diverting surplus CC to value-adding industrial reuse rather than field disposal can enhance resource efficiency without compromising soil quality or harvest yields.

Given its abundance as a residue devoid of major cultivation impacts, CC constitutes an attractive and vastly underutilized feedstock for developing bio-based industries. Global corn biometrics (Fig. 2) confirm consistent yields near 1.23 billion tons annually from 1961 to 2022, centered in prominent agricultural strongholds like the Americas and Asia; that could sustain sizeable cob biomass surpluses without disrupting food production. This stability highlights the promise of corn agriculture to provide both grain commodities and residue co-products at scale. Therefore, understanding the fiber composition of CC opens possibilities for utilizing this agricultural by-product in diverse industries, aligning with sustainable practices and contributing to the circular economy.

Materials and methods

The corn variety chosen as the raw material for this research investigation was Sammaz-16, a widely cultivated late-maturing white kernel hybrid in Nigeria, known for multiple favorable agronomic traits. Sammaz-16 reaches physiological maturity within 90–120 days after planting, enabling two seasonal harvests annually through appropriate sowing time management (Htsfarms 2022). Beyond rapid maturation, this variety possesses desirable ear and plant architectural attributes like semi-compact arrangement, cylindrical shapeliness, and medium cob positioning. Such morphological features prevent excessive lodging and maintain structural integrity despite heavy cob loading, thereby minimizing harvest and post-harvest handling losses which may exceed

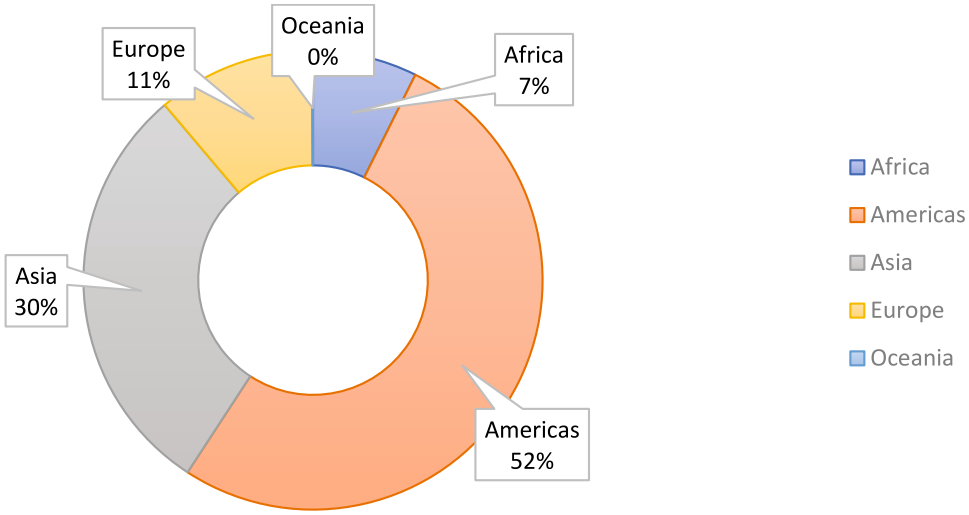

Fig. 2 Average production share of corn by region from 1961 to 2022 *Source* FAO, (2023)

10% in traditional varieties (Htsfarms 2022). Additionally, Sammaz-16 demonstrates resilience against parasitic infestations by the noxious witchweed Striga, which causes substantial grain yield declines in susceptible corn cultivars. Under heavy Striga infestation pressure, this variety experiences reduced parasitism intensity coupled with lower emerging parasite counts in contrast to older unimproved farmers' landraces. The cumulative outcome is reasonably contained productivity declines relative to intolerant genotypes, as quantified through field assessments by the commercial breeder (Htsfarms 2022). 40 Kilograms of Sammaz-16 corncobs utilized in this study were sourced from a cultivated farm situated in Makurdi, Benue State, Nigeria (Latitude 7°43'N, Longitude 8°32'E) during the October 2023 harvest season. The corncobs were obtained directly from the farm after mechanical threshing/hand milling to ensure their authenticity and minimize impurities. This was achieved by having an initial agreement with the farmers on using their waste after harvesting for research purposes. The corn was sun-dried following the normal traditional procedure and devoid of any chemical preservative and pesticides. Afterward, they were hand milled and stored in an open space for collection. Uniform-sized undamaged CC were manually selected via visual examination and transported to the laboratory. The choice of high-performing Sammaz-16 hybrid over local varieties for the research was governed by several overriding considerations beyond agronomic superiority, like year-round availability and consistency in physicochemical properties necessary for comparative analytical work. Using a commercially cultivated strain also ensures better replicability of the study instead of landraces with vague unstable genetics.

Observation of macrostructure and microstructure

Preliminary sample preparation procedures were conducted prior to microscopic visualization of the CC morphology. Physical characterization of twenty randomly selected full-length CCs (Table 1) yielded mean values of 130.2 mm (length), 26.4 mm (diameter), and 25.2 g (unit mass), giving a volume of 92.59 cm3. The CCs, harvested from local farms, were initially subjected to oven-drying at 100 °C for 45 min. This step was crucial to eliminate any residual moisture while preserving the integrity of the inherent biomass structure (Pinto et al. 2012).

The volume for each CC was calculated using the assumed volume of a cylinder: $V = \pi r^2 h$, where r is the radius (diameter/2), and h is the length. This aligns with the established protocol of Zou et al. (2021) and because the experiential samples were cylindrical in shape. The dried cob specimens were then carefully sectioned along both transverse (across width) and longitudinal (along height) planes using a band saw, creating precise radial and axial incisions. These cross sectional slices provided valuable insights into the interior arrangements of the CC, such as the distribution of vascular bundles and parenchyma spaces. In contrast, the longitudinal portions revealed the ordered stacking of fibrous and ground tissues along the vertical axes. A quantitative morphometric assessment of the key cob regions was enabled by measuring respective diameters of 3 randomly selected CC for pith cavity width (LU), woody layer width (MU), and overall external width (GU) for triplicate sections. The cross sectional area (CSA) values for the upper pith, middle sclerenchyma, and lower pericarp zones were subsequently derived using Eqs. 1, 2 and 3 as representative size fractions and shown in Table 2:

$$CU = \pi\left(\frac{GU}{2}\right)^2 \quad (1)$$

Table 1 Physical analysis of 20 randomly selected full-length corncobs

Corncob sample	Length (mm)	Diameter (mm)	Weight (g)	Volume (cm^3)
1	128.5	24.8	24.1	83.04
2	131.7	27.0	25.9	95.19
3	129.8	25.6	24.7	87.33
4	132.3	26.9	25.8	94.98
5	130.6	26.2	25.3	90.43
6	129.1	24.9	24.0	82.82
7	131.9	26.8	25.7	94.40
8	128.9	25.3	24.5	85.09
9	130.8	26.5	25.3	92.29
10	131.2	26.7	25.6	93.57
11	129.5	25.7	24.8	87.55
12	132.1	27.0	26.1	95.47
13	130.4	26.3	25.4	91.16
14	129.7	25.5	24.6	86.39
15	131.5	26.9	25.8	94.69
16	128.7	25.1	24.3	83.57
17	130.9	26.6	25.6	92.93
18	129.3	25.4	24.6	85.60
19	131.8	26.9	26.0	94.91
20	130.0	26.0	25.1	89.17
Mean	130.2	26.4	25.2	92.59
SD	1.26	0.75	0.64	4.55

Table 2 Cross section of cob area and dimension distribution

Corncob	Section	Pith (mm)	Woody ring (mm)	Glume (mm)	Cross sectional area (mm^2)
Sample A	Upper	8.95	17.75	26.30	543.12
	Middle	9.88	19.05	27.08	575.86
	Lower	12.18	19.80	28.38	632.45
Sample B	Upper	9.12	17.98	26.52	552.17
	Middle	10.08	19.25	27.28	584.11
	Lower	12.38	20.02	28.58	641.37
Sample C	Upper	9.14	17.97	26.50	551.49
	Middle	10.07	19.24	27.24	583.90
	Lower	12.37	20.00	28.57	642.07
Mean	Upper	9.07	17.90	26.44	549.26
	Middle	10.01	19.18	27.20	581.29
	Lower	12.31	19.94	28.51	638.63
SD	Upper	0.10	0.13	0.12	4.97
	Middle	0.11	0.11	0.11	4.67
	Lower	0.11	0.12	0.11	5.29

$$CM = \pi\left(\frac{MU}{2}\right)^2 \quad (2)$$

$$CL = \pi\left(\frac{LU}{2}\right)^2 \quad (3)$$

where CU, CM, and CL denote pith, woody, and annular glume CSA (mm^2) values, respectively.

The relatively low standard deviations across all measurements (e.g., 1.26 mm for length, 0.75 mm for diameter) shows a good level of consistency in the CC samples and suggest the superior agronomical property of the hybrid specie of CC. Gross-level macrostructural details of the sectioned CC samples were also documented using a TM4000Plus tabletop digital microscope system (Hitachi High-Tech Corporation, Tokyo, Japan). This advanced imaging equipment allowed for the capture of high-quality images, enabling the identification of key anatomical features and the assessment of overall structural organization. The macroscopic examination provided a foundation for understanding the CC's morphology and guided the selection of representative areas for subsequent micro-level analysis. To achieve higher-resolution micro-level assessment, scanning electron microscopy (SEM) was employed. However, this technique necessitated further sample processing to ensure optimal imaging conditions. A 6.2 mm thick cross sectional CC slice was carefully mounted on a metallic stub and secured using copper tape. To prevent specimen charging and glare during SEM imaging, the mounted surface was sputter-coated with a thin, 5 nm layer of gold–palladium

alloy in a vacuum evaporator. This conductive coating enhances the sample's interaction with the electron beam, resulting in improved image quality and resolution. The SEM imaging was conducted using a Carl Zeiss EVO LS 10 system (Carl Zeiss Microscopy GmbH, Jena, Germany) under variable pressure mode. An acceleration voltage of 15 kV and a probe (beam) current of ~ 100 pA were applied across a working distance of 10 mm, which allowed for the generation of high-quality images and elemental spectra. Multiple fields were examined at various magnifications ranging from 25 × to 1000 × under high vacuum, ensuring the capture of representative microstructural features. The SEM analysis provided detailed insights into the microstructure of the CC, revealing the arrangement and morphology of individual cells, cell walls, and other microscopic components. The high-resolution images allowed for the identification of key features such as pits, vessels, and fibers, which play essential roles in the biomass physical and mechanical characteristics.

Mechanical testing

To assess the biomechanical attributes of CC biomass, axial compression and tensile strength quantification were performed using a universal material testing equipment. The Instron 34TM-50 system, coupled with Bluehill Universal software (Illinois Tool Works Inc., Norwood, MA, United States), was employed to conduct axial compressive and tensile testing on CC samples. This instrument is equipped with a 50 kN load cell and integrated with Bluehill Universal software, ensuring precise control and data acquisition during testing. The load cell used in this system has a capacity of 50 kN (11,250 lbf) and boasts a high degree of accuracy (± 0.5% of reading down to 1/500th of load cell capacity). Prior to mechanical testing, CC samples were prepared following the biomass evaluation protocols of Zou et al. (2021) to ensure consistency. Each cob was cut into multiple segments, allowing paired experiments across different regions. For compression testing, 9 samples were prepared (3 from 1 CC). From each cob, 3 transverse slices, 30 mm thick, were taken from the upper, middle, and lower sections. This sampling strategy ensured coverage of the entire cob structure and reduced the influence of localized variations. During crushing, care was taken to align the cylindrical samples correctly with the applied load, as proper orientation is essential to avoid uneven stress distribution and inaccurate results. For tensile testing, another 9 samples (three per cob) were prepared. Axial quadrant segments, 80 mm long, were excised parallel to the vascular bundles. This orientation enabled assessment of fiber-level tensile behavior along the CC primary structural axis. The specimens were mounted in the pneumatic wedge grips of a universal testing machine

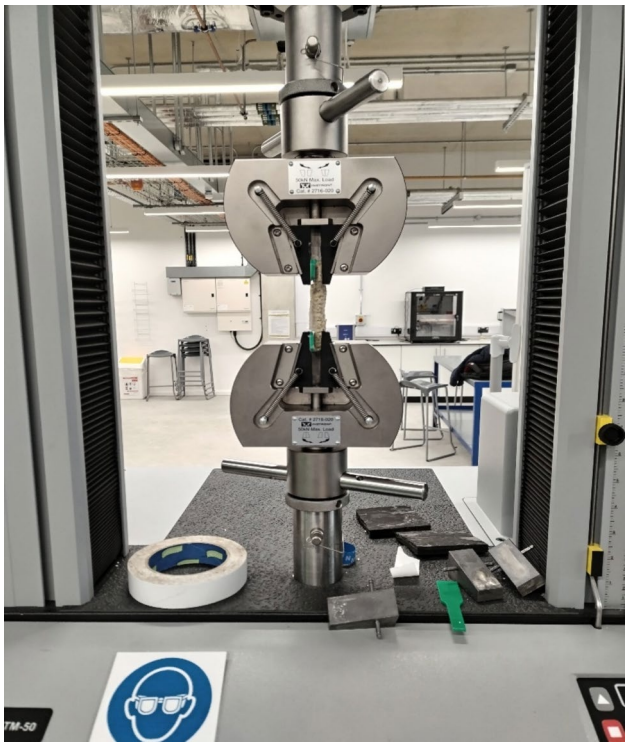

Fig. 3 Tensile testing of Corncob

(see Fig. 3). Tests were conducted at a constant crosshead displacement rate of 0.02 mm/min under ambient room temperature, and the failure patterns were documented using a digital camera. The stress–strain graphs were obtained and the following parameters such as yield strength, Young's modulus, and fracture limits were automatically extrapolated from the Bluehill Universal software.

Determination of fiber and starch content

The determination of fiber contents in the experimental samples was carried out using a combination of gravimetric analysis and modified detergent methods. The approach was adapted from the work of Van Soest et al. (1991) and involved a series of steps to accurately quantify the desired components. The first stage of the process involved the application of the modified neutral detergent fiber (NDF) method, which allows for the collective quantification of cellulose, hemicellulose, and lignin. This was followed by the acid detergent fiber (ADF) method, which specifically targets cellulose and lignin. The principle behind these methods relies on a sequence of gravimetric analyses, including hot filtration, extraction using organic solvents, and thorough drying of the samples. The final step in this phase involved the determination of the ash content of the processed samples, as described by Pointner et al. (2014). To further refine the quantification process and obtain a more

precise measurement of cellulose content, a direct determination approach was employed in place of the conventional Acid Detergent Lignin (ADL) method. This innovative technique, developed by Horwitz & Latimer (2005), involved a hot liquid extraction procedure using a combination of acetic acid, nitric acid, and organic solvents. The extracted solution was then subjected to filtration to isolate the cellulose component. The hot liquid extraction process was performed using an acid detergent solution, following the methodology outlined by Horwitz & Latimer (2005) and Neumann & Basler (1976). This step was crucial in ensuring the complete dissolution of non-cellulosic components, allowing for the accurate quantification of cellulose content. The resulting solution was then filtered using an organic solvent to obtain a pure cellulose fraction. With the cellulose content directly determined, the hemicellulose and lignin contents were calculated using simple arithmetic based on the NDF and ADF values. The hemicellulose content was obtained by subtracting the ADF value (representing cellulose and lignin) from the NDF value (representing cellulose, hemicellulose, and lignin). This difference represents the quantity of hemicellulose present in the sample. Similarly, the lignin content was indirectly determined by calculating the difference between the ADF value (lignin and cellulose) and the directly measured cellulose content. This approach provides a more accurate estimation of lignin content compared to the conventional ADL method.

In addition to the fiber analysis, the starch content of the chopped corncobs was determined using the Total Starch (AA/AMG) Assay Kit. This specialized kit, which follows the AOAC Method 996.11 and AACC Method 76–13.01, provides a reliable and standardized approach for quantifying starch in various matrices. The assay involves the enzymatic hydrolysis of starch to glucose, followed by the colorimetric determination of glucose concentration. The use of the Total Starch Assay Kit offers several advantages over traditional methods for starch quantification. It provides a high level of specificity and sensitivity, ensuring accurate results even in the presence of interfering compounds. Moreover, the kit's standardized protocol allows for reproducibility and comparability of results across different studies and laboratories.

To determine the pectin content in corncob, a multi-step process was employed, using the collected CC sample. The cleaned corncobs were dried in a forced-air oven at 60 °C for 24 h. Once dried, the corncobs were ground into a fine powder using a mill to ensure particle size uniformity. The powdered material was passed through a 60-mesh sieve to obtain a homogeneous sample. For the extraction phase, 5 g of the powdered corncob sample was weighed into a 250 mL Erlenmeyer flask. To this, 100 mL of 0.05 M hydrochloric acid (HCl) was added, and the mixture was heated to 85 °C while stirring constantly for 1 h. After heating, the mixture was cooled to room temperature and filtered through Whatman No. 1 filter paper. The pectin was then precipitated by adding 95% ethanol to the filtrate in a 1:2 ratio (filtrate). The mixture was allowed to stand for 1 h, during which the pectin precipitated. The precipitate was collected by filtering through pre-weighed filter paper and subsequently washed with 70% ethanol to remove impurities. In the drying and weighing stage, the filter paper containing the pectin precipitate was dried in an oven at 50 °C until a constant weight was achieved, approximately 4 h. The dried sample was cooled in a desiccator and weighed to determine the pectin yield. Finally, the pectin content was calculated using the formula: Pectin content (%) = (Weight of dried pectin / Weight of corncob sample) × 100.

Results and discussions

Macrostructure of Corncob

The CC consists of the central, cylindrical rachis upon which kernels are attached. It harbors the carpopodium, ensuring organized kernel arrangement across the cob surface, influencing nutrient transmission into developing kernels. Macroscopic examination reveals a rigid, skeletal cob structure with cylindrical symmetry. However, detailed geometric analysis indicates a slight conical shape, with gradient distributions in cross sectional dimensions from the cob base to apex. In order to characterize axial geometric properties, cross sections were excised from the top, middle, and lower parts, as depicted in Fig. 4. Results demonstrate measurable differences in cob diameter and thickness-related parameters in an apico-basal direction, congruent with its overall cylindrical morphology. Further quantitative delineation of CC architecture and kernel attachment patterns elucidates underlying transport mechanisms supporting grain development and nutrient deposition within the mature kernel.

The CC possesses a distinctive macro-morphology with three concentric layers that are visually discernible owing to differences in coloration, texture, and structural density. As evidenced in Fig. 4 from the exterior to the interior reveals a thin external flaky covering called the annular glumes or outer pericarp. This transitions into the prominently thicker sclerenchymatous ring known as the "woody layer" or "ring" which provides primary mechanical support. The innermost section is comprised of parenchymatous pith tissue and contributes mainly to metabolic transport functions. Cross sectional examination undertaken in this study consistently showed CC tissue strata arranged as irregular circular bands across the transverse width. Quantitative morphometric assessment of the key cob regions is shown in Table 2.

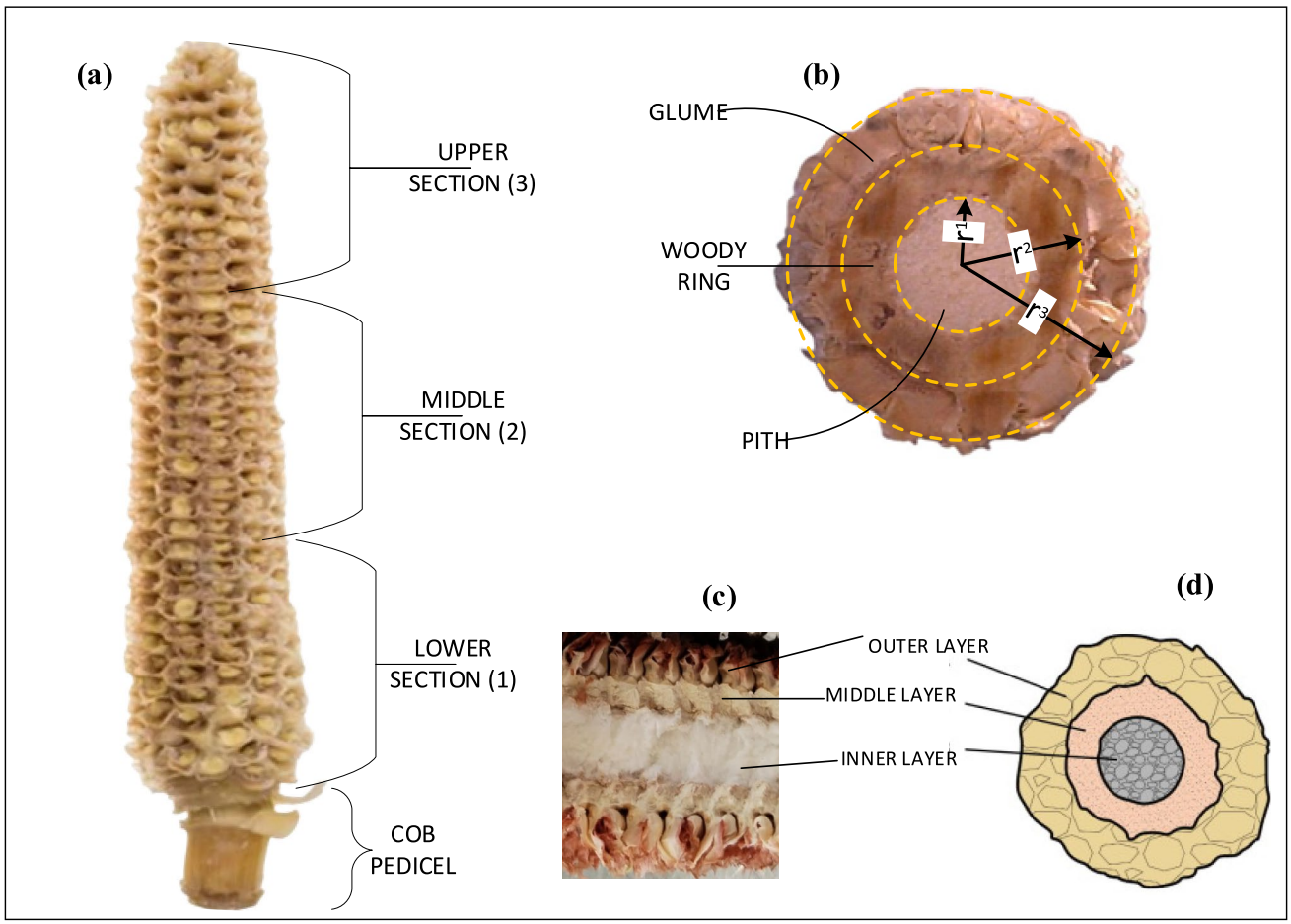

Fig. 4 Macrostructure of CC. (**a**) Sample of some dried cobs collected for the experimental tests. (**b**) Transverse section. (**c**) Longitudinal section of a corncob and (**d**) Structural stratification in corncob cross sections (Bovo et al. 2022)

Microstructure of corncob

From a biomaterial engineering perspective, the mechanical strength and performance profile of agricultural residues like CCs is determined not just by material composition but also the inherent structural arrangement of various fractions. SEM was utilized to characterize the intricate microstructure across CC anatomical sections. Imagery validated macro-scale observations of distinct morphological differences along the layers, further substantiating significant variability at a microscopic level. The differentiated components as seen in Fig. 5-Fig. 7 include a flaky and porous outer annular glumes pericarp of degenerate tissue encasing the prominently thicker and wood-like middle sclerenchyma ring, which provides stiffness and supports the soft vascularized inner pith. Such disparities in texture and void concentrations critically dictate compressive, tensile, or shearing mechanics through varied degrees of compressibility and susceptibility to fracture propagation. These trends were endorsed by SEM micrographs of the cob cross section that, when magnified, clearly evidenced the divergent microstructure between middle woody and innermost parenchyma sections, as described by Anandjiwala et al. (2008) and Pinto et al. (2012). Micro and macro-scale morphological characterizations in this study affirm observations by past researchers that, despite regional differences, CC biomass represents a highly ordered heterogeneous organic composite system, and the fundamental characteristics defining this material are typically consistent and repeatable. Therefore, CC architecture exerts significant reinforcement outcomes that contribute to stress accommodation and load distribution when subjected to external forces. The different morphologies of the CC confer to the whole material very particular properties and are discussed in the following sections.

Pith

The central core of the cob (pith) exhibits an airy structure characterized by delicate layers of film-like material (cell wall) organized to create cavities and porous formations.

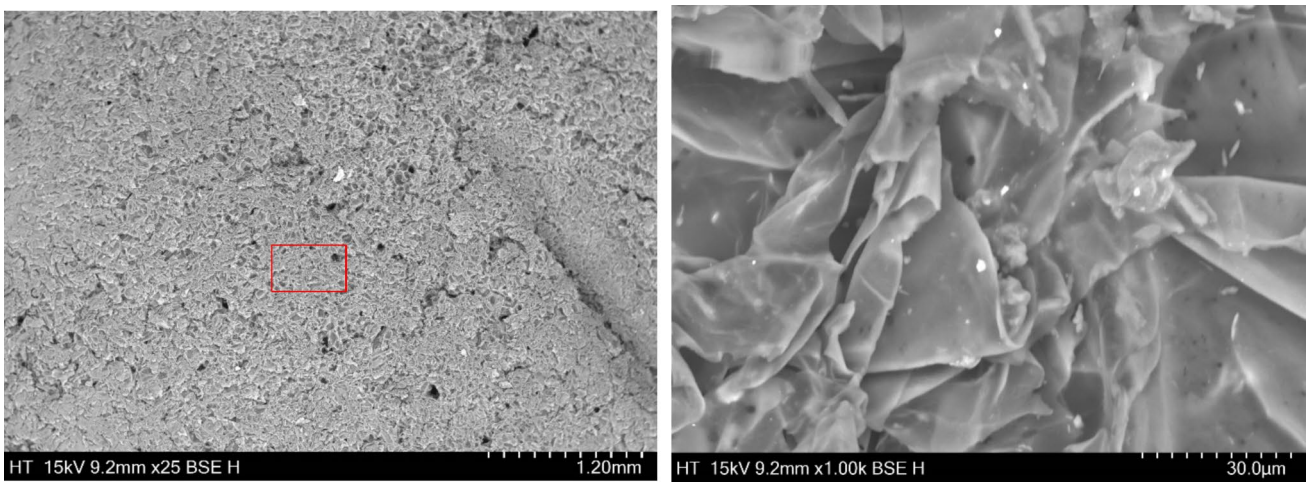

Fig. 5 SEM image of CC pith (**a**) × 25 magnification and (**b**) × 1.00 k magnification

The tissue structure is sponge-like and homogeneous in nature; having cells shaped like an irregular ellipse and their cells networked without gaps. Under external pressure, the sponge-like composition distributes the force evenly among the cells made up of numerous small perforations and cellulose fibril strands. It exhibits low density with high water retention capability resulting in its compressible and pliable nature owing to air spaces and closed cell walls. For building and construction applications, this porous microcomposition is a good resistive property required for strength and durability. Also, the pith is intriguing to examine from a thermal perspective, given its possible use as insulation in buildings.

In Fig. 5a (× 25 magnification), a wider view shows a honeycomb-like arrangement of the pith with numerous small cavities, and the structure appears relatively uniform across the field of view, suggesting consistent properties throughout. Some micro-cracks or fissures are evident, which could influence fracture behavior and overall strength; the pith comprises very small, interconnected particles that form a complex network of solid material and void spaces; and the overall surface is rough and uneven, a characteristic that may enhance bonding in composite applications. At higher magnification in Fig. 5b (× 1.00 k), the pith exhibits a layered, sheet-like structure with overlapping plates that likely contribute to compressibility and resilience; visible gaps and voids between the layers indicate high porosity, underpinning the material's light weight and potential insulating performance; the sheets display a relatively smooth surface with local irregularities that could affect interactions with binders or adjacent phases in composites; the layers are interconnected at various points, which may contribute to overall structural integrity; and the sheet thickness varies, implying non-uniform mechanical properties across the pith.

Relating these observations to the mechanical attributes and potential use as SBMs:

i. *Lightweight structure* The highly porous nature of the pith, evident in both images, contributes to its low density. This makes it an excellent candidate for lightweight building materials, insulation, or as an aggregate in lightweight concrete.
ii. *Compressibility* The layered structure in Fig. 5b suggests good compressibility, which could be beneficial for applications requiring energy absorption or cushioning properties.
iii. *Thermal and acoustic insulation* The numerous air pockets and porous structure observed in both images indicate excellent potential for thermal and acoustic insulation applications.
iv. *Moisture absorption* The open, interconnected structure suggests high moisture absorption capacity, which could be advantageous for humidity regulation in buildings but may require treatment for water-sensitive applications.
v. *Mechanical strength* While the pith structure appears less rigid than the woody ring or glume, its interconnected network could provide some degree of structural integrity.
vi. *Composite reinforcement* The rough surface texture and complex structure could provide good mechanical interlocking with matrix materials in composites, potentially enhancing the overall strength and toughness of the composite.
vii. *Anisotropic properties* The layered structure in Fig. 5b suggests that the pith may exhibit different properties in different directions. This could be exploited in design to optimize performance for specific applications.

viii. *Cellular material behavior* The honeycomb-like structure in Fig. 5a is reminiscent of engineered cellular materials, suggesting that the pith could exhibit similar mechanical behaviors, such as good energy absorption under compression.

ix. *Biodegradability* The organic nature of the pith structure indicates that it would be biodegradable, aligning with sustainable building practices and end-of-life considerations for materials.

Woody ring

This structure typically comprises a matrix of cells characterized by diverse elements, such as cellulose, hemicellulose, and lignin, forming a complex network. Within this network, various features are observable, including vessel elements, fibers, and parenchyma cells. These elements collectively contribute to the strength and rigidity of the corncob's woody ring. The arrangement of cellulose microfibrils and lignin within the cell walls provides structural support, while the presence of small cavities and micro-channels allows for fluid exchange and transport of nutrients accounting for high structural density. The microstructure's configuration determines the CC's mechanical properties, resilience to external pressures, and overall functionality within its natural environment.

In Fig. 6a (×25 magnification), the woody ring displays a highly textured, uneven macro-scale topography, with visible cracks and fissures that indicate potential crack-propagation paths and may influence fracture behavior; the surface is peppered with smaller particles, likely remnants of the corncob's cellular structure or processing artifacts. The pronounced heterogeneity suggests that material properties vary across regions of the ring. In Fig. 6b (×1.00 k magnification), which offers a more detailed view of the CC woody ring's surface, a complex network of interwoven fibers characteristic of corncobs is evident; these fibers are likely composed of cellulose and lignin, conferring strength and rigidity, and they are arranged in multiple layers that help the material resist mechanical stresses from different directions. The micrograph also shows gaps and pores between fibers, indicating porosity that can affect density, thermal insulation, and acoustic absorption, while the irregular fiber surfaces increase overall surface area and could therefore enhance bonding when the material is used in composite applications.

Relating these observations to the mechanical attributes and potential use as SBMs:

i. *Strength and stiffness* The fibrous structure observed in Fig. 6b suggests that the woody ring possesses good tensile strength and stiffness. The multi-directional arrangement of fibers could provide resistance to various types of mechanical loads, making it suitable for reinforcement in composite materials.

ii. *Lightweight structure* The presence of pores and gaps between fibers indicates that the woody ring is naturally lightweight, which is advantageous for reducing the overall weight of building materials without compromising strength.

iii. *Thermal and acoustic insulation* The porous nature of the material, as seen in both images, suggests good potential for thermal and acoustic insulation. The air pockets trapped within the structure can help reduce heat transfer and absorb sound waves.

iv. *Moisture absorption and desorption* The fibrous and porous structure likely allows for efficient moisture

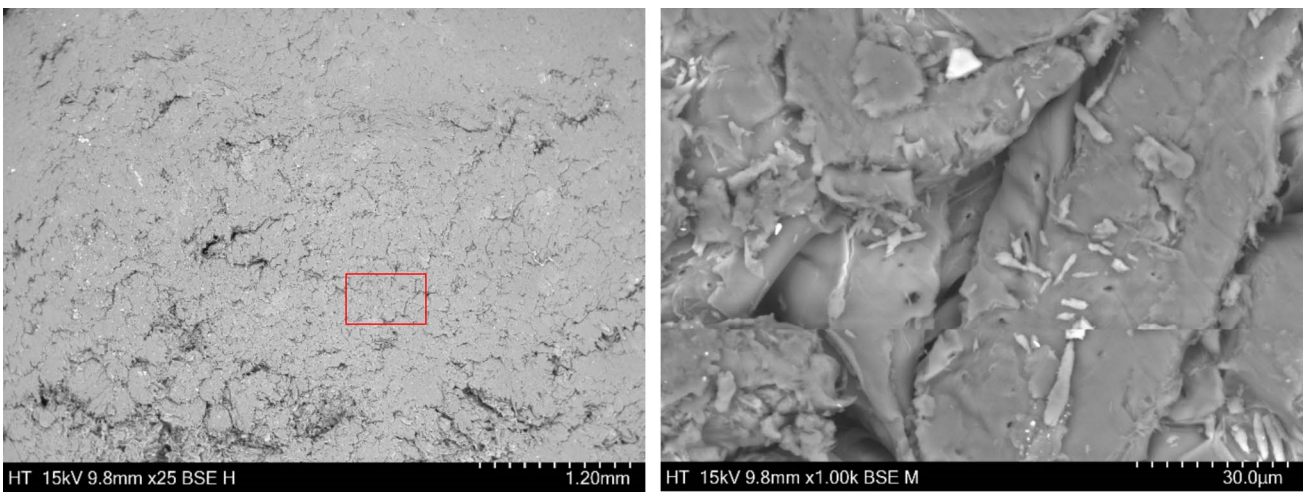

Fig. 6 SEM image of CC woody ring (**a**) ×25 magnification and (**b**) ×1.00 k magnification

absorption and desorption, which could be beneficial for regulating humidity in indoor environments.

v. *Interfacial bonding* The rough surface texture and high surface area observed in both images indicate good potential for interfacial bonding with matrices in composite materials, which could lead to improved mechanical properties of the final product.

vi. *Anisotropic properties* The layered arrangement of fibers suggests that the material may exhibit anisotropic behavior, with different mechanical properties in different directions. This could be exploited in design to optimize performance for specific applications.

vii. *Fracture behavior* The presence of cracks and fissures in Fig. 6a provides insights into the material's fracture mechanics. Understanding this behavior is crucial for predicting and improving the durability of building materials made from corncob woody rings.

Glume

Under microscopic observation, the glume layer exhibits a fibrous and layered structure, often showing intricate patterns and arrangements of cells, with a surface that displays a textured or irregular appearance. This is the most complex concerning morphology, as it exhibits both a filamentous and dense appearance with holes and cavities. The cells are elliptically protruded, also forming a porous sponge-like tissue structure of low density similar to pith. Transparent glandular hairs are visible at the interface between the inner glume and the woody ring. The complexity in morphology contributes to influence the layer's strength and resilience.

Figure 7a provides a broader view of the corncob glume surface. The texture is marked by numerous small, dot-like features that give a distinctly textured appearance and increase surface area. This attribute improves bonding with other materials in composite applications. A central cluster of fibrous elements is evident; these fibers are likely cellulose-based and contribute substantially to tensile strength. The image also suggests a layered, laminated architecture that can enhance resistance to bending and shear forces. Several micro-cracks or fissures are visible (whether natural or introduced during sample preparation), and recognizing these features is important for predicting failure modes and planning appropriate reinforcement strategies. By contrast, Fig. 7b presents a cross sectional, cellular-level view, revealing a honeycomb-like array of cells of varying sizes and shapes that confer low weight while maintaining structural integrity. The cell walls appear relatively thick, consistent with good mechanical strength and typically associated with higher compressive and tensile capacities. White regions indicate pore spaces or voids within the structure, which are integral to thermal insulation and the material's ability to absorb sound and moisture. Some cells are interconnected, facilitating stress transfer through the network and potentially improving the overall mechanical performance of the glume.

Relating these observations to the mechanical attributes and potential use as SBMs:

i. *Lightweight structure* The cellular nature of the glume contributes to the lightweight characteristics of corncobs, making them attractive for applications where weight reduction is important, such as in insulation or lightweight concrete aggregates.

ii. *Mechanical strength* The thick cell walls and fibrous elements suggest good mechanical properties, particularly in terms of compressive and tensile strengths. This could make corncob-derived materials suitable

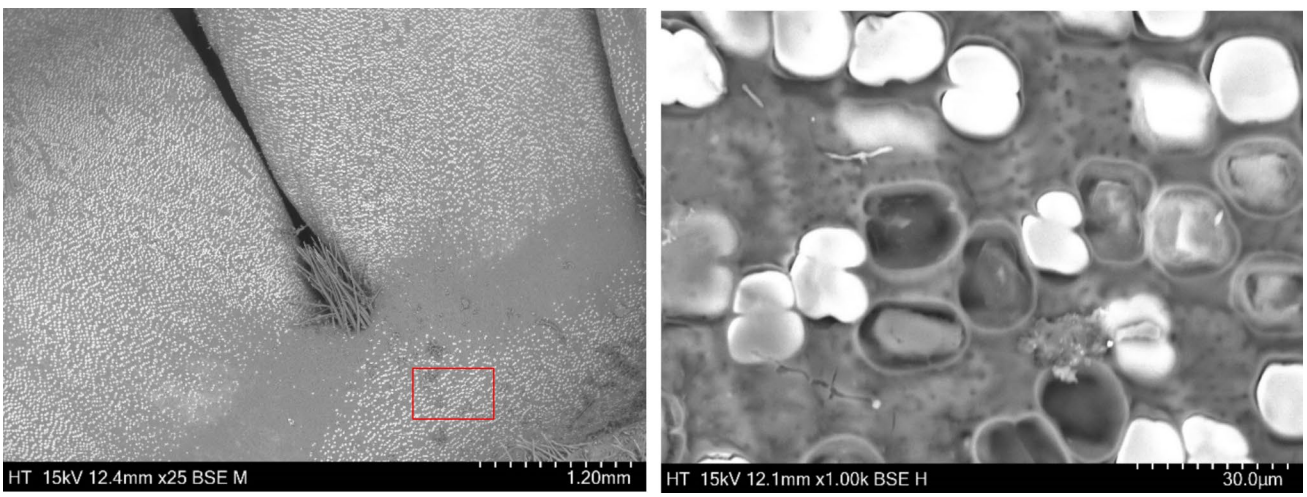

Fig. 7 SEM image of corncob glume, (**a**) × 25 magnification and (**b**) × 1.00 k magnification

for load-bearing applications or as reinforcement in composites.

iii. *Insulation properties* The porous structure observed in Fig. 7b indicates good potential for thermal and acoustic insulation. The air pockets trapped within the cellular structure can effectively reduce heat transfer and absorb sound waves.

iv. *Moisture absorption and regulation* The porous nature also suggests good moisture absorption capabilities, which could be beneficial for humidity regulation in building interiors.

v. *Surface bonding* The textured surface seen in Fig. 7a could provide good adhesion properties, potentially enhancing the material's ability to bond with matrices in composite materials or with other building elements.

Elemental composition of corncob

The desired qualities and suitability of CC for building and construction purposes are influenced not only by its physical structures at both macro and micro-levels but also by its elemental composition, particularly the fibrous components. These fiber constituents vary in content and distribution across the pith, woody ring, and glume, indirectly impacting the corncob's overall properties. Energy Dispersive Spectroscopy (EDS) is a dependable method used to analyze the elemental composition of materials by detecting characteristic X-rays emitted when exposed to high-energy electrons. SEM data aid in understanding the material's chemical composition, assisting researchers in characterizing materials, identifying impurities, and evaluating their suitability for specific applications. Figure 8 shows the results obtained from SEM analysis, depicting the elemental composition of CC.

EDS analysis revealed distinct elemental distributions across the three anatomical regions of the corncob structure. The pith showed predominant carbon (67.74%) and oxygen (31.22%) content, with minor concentrations of potassium (0.68%), silicon (0.18%), and chlorine (0.15%). This composition aligns with its cellular structure optimized for metabolic transport. The woody ring exhibited similar carbon–oxygen dominance but with reduced trace elements, reflecting its dense mechanical support function. Most notably, the glume displayed enhanced silicon (2.52%) and aluminum (0.69%) content, suggesting natural reinforcement properties. These elemental variations across layers directly influence the material's mechanical and functional characteristics. Elements in CC include:

a) *Ba (Barium)* Detected in trace amounts (0.02%) and likely originating from environmental or incidental sources. It may contribute to the overall composition.

b) *Pb (Lead)* Present in minimal quantities (0.01%) is a known environmental contaminant and can be associated with various sources like dust, soil, or industrial emissions.

c) *Sb (Antimony)* Detected in extremely low amounts (0.00%), suggesting minimal or negligible presence. It is crucial to note that its absence might result from limitations in the detection sensitivity of the instrument.

d) *C (Carbon)* Forms the major component of the sample, constituting about 64–67% of the composition. Carbon is ubiquitous in organic materials, which could indicate the sample's organic nature.

e) *O (Oxygen)* Comprises 31–34% of the sample. Oxygen is prevalent in most inorganic and organic compounds, forming a significant part of the sample's composition.

f) *K (Potassium)* Detected at a relatively low percentage (0.31–0.68). Potassium is a common element in many natural materials, including minerals, plants, and living organisms.

g) *Si (Silicon)* Found in very small quantities (0.18%). Silicon is a common element in minerals and is often present in various compounds.

h) *Cl (Chlorine)* Present in trace amounts (0.15%). This element likely originates from environmental salts or nutrient residues.

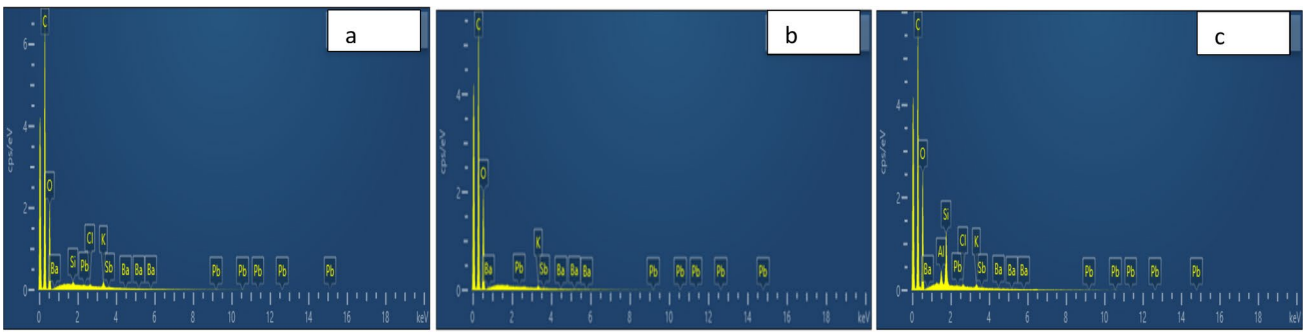

Fig. 8 Map spectrum of corncob: **a** pith; **b** woody ring; **c** glume

Table 3 Elemental composition of CC

CC layer	Element	Line type	Weight %	Weight % Sigma	Atomic %
Pith	Ba	L series	0.02	0.08	0.00
	Pb	M series	0.01	0.09	0.00
	Sb	L series	0.00	0.06	0.00
	C	K series	67.74	0.26	74.02
	O	K series	31.22	0.25	25.61
	K	K series	0.68	0.03	0.23
	Si	K series	0.18	0.02	0.09
	Cl	K series	0.15	0.02	0.06
	Total		100.00		100.00
Woody ring	Ba	L series	0.06	0.09	0.01
	Pb	M series	0.00	0.11	0.00
	Sb	L series	0.00	0.07	0.00
	C	K series	65.58	0.37	71.88
	O	K series	34.05	0.37	28.01
	K	K series	0.31	0.03	0.10
	Total		100.00		100.00
Glume	Ba	L series	0.02	0.10	0.00
	Pb	M series	0.00	0.12	0.00
	Sb	L series	0.05	0.08	0.01
	C	K series	64.73	0.42	71.97
	O	K series	31.54	0.40	26.33
	Si	K series	2.52	0.05	1.20
	Al	K series	0.69	0.04	0.34
	K	K series	0.30	0.04	0.10
	Cl	K series	0.15	0.03	0.06
	Total		100.00		100.00

i) *Al (Aluminum)* Detected in minor amounts due to its growth-limiting abilities in corn.

Table 3 represents the elemental composition obtained from the map sum spectrum analysis. The elements are identified based on their characteristic X-ray emissions when the CC sample was bombarded with high-energy electrons.

The "Weight % Sigma" values represent the standard deviation or uncertainty associated with the measured percentages. Higher values suggest a wider range of possible values around the reported percentage, particularly noticeable in Carbon (C) and Oxygen (O). The element composition of pith, woody ring, and glume has a dominant and trace element.

- *Dominant elements* Carbon and Oxygen collectively make up a significant portion of the samples. Their dominance, detected through the K series line, suggests the presence of organic or carbon-based compounds as well as oxides in the sample material.
- *Trace elements* Elements like Barium, Lead, and Antimony, though present in minute quantities, might have implications for the sample's origin, environmental exposure, or geological composition.

Implications for material property and construction use

The high carbon content suggests the presence of organic compounds, potentially imparting lightweight, flexibility, resilience, and possible biodegradability; attributes that are advantageous for certain construction applications. The presence of oxygen, likely in the form of oxides, may enhance stability and durability, which is important for long-term use. Silicon and aluminum, although present only in minor amounts, could contribute to strength and resistance to environmental factors; both elements occur in common construction materials such as concrete and ceramics. Silicon dioxide

(silica) is a common constituent of many construction materials that supports strength and durability. The absence of heavy metals such as lead is beneficial, aligning with safety standards and environmental regulations. Antimony was detected in very low concentrations (0.00%–0.05%) in the CCs and, at these trace levels, is unlikely to have a significant effect on fire or heat resistance. Similarly, the impact of barium at low concentrations on the material's properties, including strength, is likely to be negligible. Finally, the presence of potassium contributes to the material's structural and compositional attributes, while chlorine contributes to its reactivity.

Mechanical properties of Corncob

Axial compression

The compressive strength (CS) of a CC measures its ability to withstand pressure without collapsing or experiencing structural failure, which is critical for applications such as building and composite materials. The stress–strain curves (Fig. 9) and CS results (Tables 4 and 5) clearly demonstrate distinct behavior across the upper, middle, and lower sections of the corncob. These differences reflect the heterogeneous anatomy of the cob, particularly the varying proportions of pith, woody ring, and glume tissues.

In the early stages of loading, all samples displayed a nearly linear stress–strain response as the porous pith and glume layers provided a buffering effect against applied force. Once this initial resistance was overcome, the woody ring dominated the load-bearing response until failure

Table 4 Compressive Strength result

Corncob Section	Sample ID	max Strain (%)	max Stress (MPa)
Lower	1	33.72	18.6
	2	50	21.43
	3	40.6	23.76
	average	41.44 ± 6.67	21.26 ± 2.11
Middle	1	71.76	63.88
	2	68.37	48.75
	3	58.34	84.84
	average	66.16 ± 5.70	65.82 ± 14.80
Upper	1	73.95	121.25
	2	37.91	119.3
	3	60	106.61
	average	57.29 ± 14.84	115.72 ± 6.49

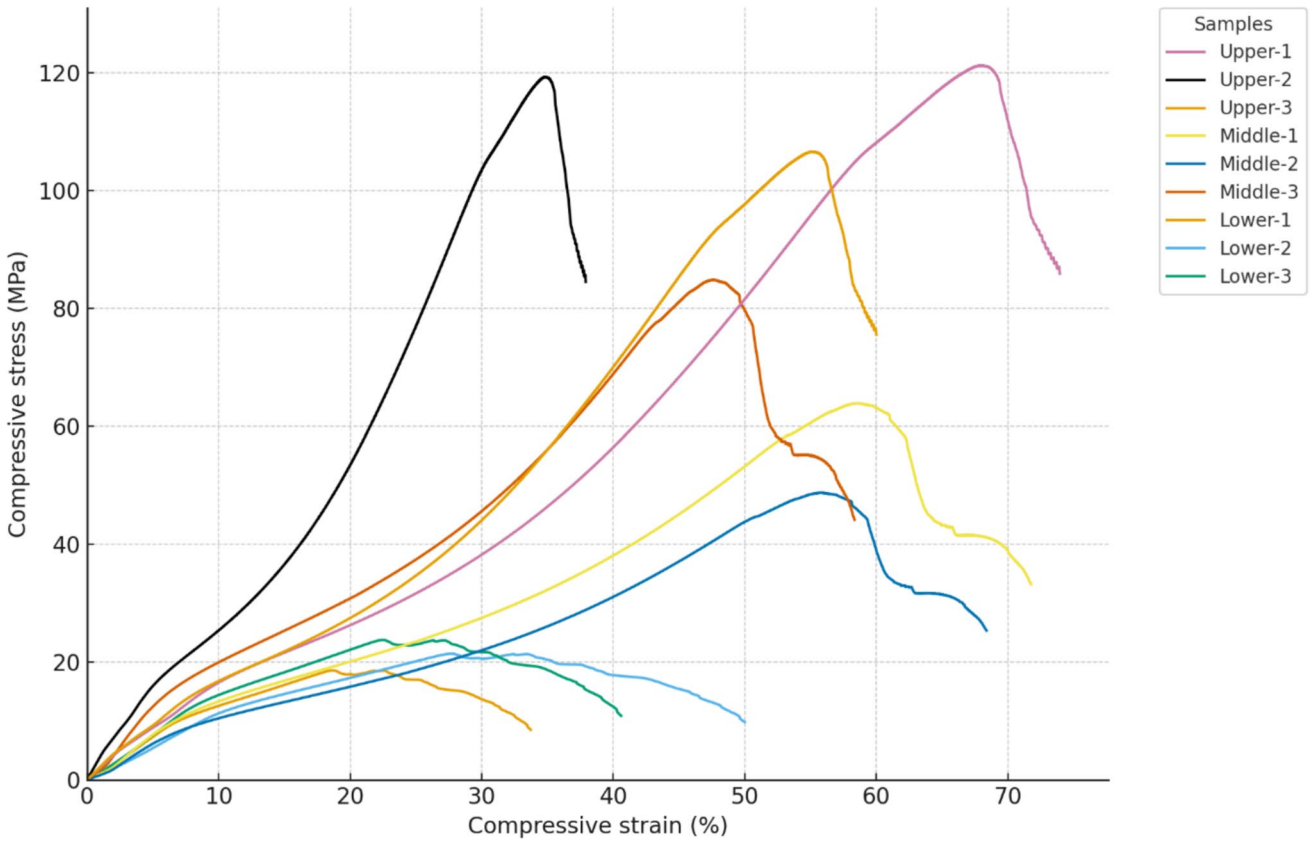

Fig. 9 Compressive strength graph

Table 5 Descriptive statistics of axial compression

Variable	Lower section	Middle section	Upper section	Mean	StDev	CoefVar	Skewness
CS at max force (MPa)	21.26	64.83	116.72	67.60	47.84	70.76	0.70
Max force (kN)	2.56	7.81	14.06	8.14	5.78	71.05	0.71
Displacement (mm)	5.62	11.54	14.32	10.49	4.44	42.35	-1.00

occurred. In all cases, failure initiated along radial lines originating from the pith and propagated outward to the glume, confirming the pith's role as the weakest link under compression.

The quantitative results show that the lower section exhibited the lowest compressive resistance, with an average strength of 21.26 ± 2.11 MPa at a strain of ~ 41%. This is consistent with its higher proportion of spongy pith, which, while efficient in dissipating pressure, transmits force rapidly to surrounding tissues and fails earlier. By contrast, the middle section demonstrated significantly higher CS, averaging 65.82 ± 14.80 MPa, with peak strains exceeding 66%. The superior behavior of this region is attributed to a denser packing of vascular bundles and a thicker woody ring. The upper section achieved the highest CS overall, averaging 115.72 ± 6.49 MPa, at displacements of up to 14 mm. This contradicts the intuitive assumption that the basal (lower) section would be stronger; instead, the upper section's denser woody ring and reduced pith content provided superior structural integrity.

Table 5 supports these findings, indicating that the upper section not only carried the highest maximum force (14.06 kN) but also exhibited the greatest stress at maximum load (116.72 MPa). In contrast, the lower section failed at much lower loads (~ 2.56 kN). Skewness and coefficient of variation values also reveal greater consistency in the mechanical response of the upper and middle sections compared to the highly variable behavior of the lower section. From an applications standpoint, the overall average CS (≈67.6 MPa) positions CC competitively among natural biomaterials. Ramos et al. (2021) showed that CC-based particleboards can meet thermal and mechanical service requirements for building envelopes, with life cycle advantages; this sectional data offer a materials-by-design lever: upper/middle fractions (woody-rich) are better suited for load-sharing cores or skins in bio-composites, whereas lower (pith-rich) fractions can be mapped to insulative, energy-absorbing layers where CS is secondary to low density and porosity.

Mechanistically, the trend agrees with fiber architecture arguments widely reported for natural fibers. Reddy & Yang (2005b) linked improved compressive performance to higher cellulose content, thicker cell walls, and lower microfibril angle, features more prevalent in woody tissues than pith. Zou et al. (2021) further demonstrated that microstructural heterogeneity in CC governs compressive response; while their focus was bulk compression, this section-resolved data sharpen that conclusion by showing that anatomical stratification (upper vs. middle vs. lower) is a dominant source of variability. In addition, the stress–strain curves exhibit an initial quasi-linear regime followed by progressive yielding and a precipitous drop at peak. When benchmarked against other residues, the average value (> 50 MPa for wheat/rice straw; < 93 MPa for bagasse) is consistent with the lignification gradient hypothesis (Reddy & Yang 2005b; Sabeen et al. 2013): bagasse, being more heavily lignified and fiber-dense, outperforms CC in compression; straw, with thinner walls and higher lumen fraction, underperforms. This triangulation supports the interpretation that woody ring continuity and fiber packing explain the upper section advantage. Moreover, the coefficient of variation observed (Table 5) is highest in the lower section, echoing Pinto et al. (2012) who cautioned that pith heterogeneity increases scatter in mechanical metrics and should be controlled by fractionation prior to product fabrication. Recent work on Foxtail palm fruit fibers shows that fiber morphology and chemistry (cellulose crystallinity, surface features, and antibacterial activity) map directly to mechanical/functional performance (Raja et al. 2024b). In CC system, prioritizing woody-rich upper/middle CC fractions for stiffness critical roles and routing pith-rich fractions to energy-absorbing/insulating layers mirrors that structure–property logic; moreover, coupling CC with fruit- or leaf-derived fibers of complementary ductility (as in Foxtail palm studies) could balance strength vs. extensibility and add functional benefits (e.g., bioactivity) in hybrid laminates.

Complementary work using numerical models (Yan 2017; Tao & Wei 2020) reproduced macroscopic impact and crushing responses of CC by treating the cob as a radially graded cellular solid; a modeling choice that implicitly assumes the same hierarchy we measured experimentally. This section-specific data provides empirical parameters that can tighten those models (e.g., section-dependent strength plateaus and strain at densification), enabling more predictive design of CC-filled cores and energy-absorbing elements. Relative to wood species, the overall average (67.6 MPa) sits within the broad range reported for softwoods/hardwoods under parallel-to-grain compression (30–80 MPa depending on density/lignin; Kaw 2005), but with notable anisotropy and localization driven by the pith–ring architecture. This suggests CC can substitute for moderate grade woods in non-critical

compressive roles, particularly where mass-specific performance and thermal/acoustic co-benefits are valued, an inference consistent with Ramos et al. (2021). This results' implication indicates that (i) sectional sorting is an actionable pathway to reduce variability and tailor properties; (ii) upper/middle fractions are promising for compressive load-sharing in bio-composites; and (iii) integrating microstructure-aware DoE (design of experiments) with SEM–EDS metrics will enable stronger structure–property correlations than bulk tests alone.

Tensile test

The tensile stress–strain curves for the CC samples (Fig. 10) highlight the anisotropic response of the material under tensile loading. Each sample set (A–C, triplicates) represents a radial quadrant segment of the cob, enabling assessment of sectional variability in mechanical response. Tensile behaviour is an essential parameter for evaluating elongation capacity, ductility, and durability of bio-based materials. Materials with higher tensile strength are better able to withstand stretching forces before failure, making them more suitable for construction or composite applications where resilience under tensile loads is critical.

The stress–strain curves display a characteristic pattern of lignocellulosic materials: a steep initial elastic rise, a peak stress point, and subsequent strain-softening. This progression indicates that CC tissues can store elastic energy before microstructural yielding, after which fiber pull-out, sliding, and intercellular debonding dominate. Microstructural observations explain a sectional variability in CC. The pith-rich middle zones behave like cellular foams, where deformation occurs through cell wall bending and collapse, giving high ductility but limited strength. The woody ring-dominated upper zones have thicker cell walls, lower microfibril angles, and higher lignification, conferring strength and stiffness but greater brittleness. Meanwhile, glume tissues exhibit strong fiber bonding, delaying detachment but ultimately transmitting stresses into the woody ring, where brittle fracture initiates. The tensile and compression behaviors can be rationalized by fracture mechanisms commonly observed in lignocellulosic composites. In the pith-rich zones, failure proceeds by cell wall bending, lumen collapse, and fiber sliding, which explains the higher strains at lower stresses. In contrast, the woody ring zones fail by

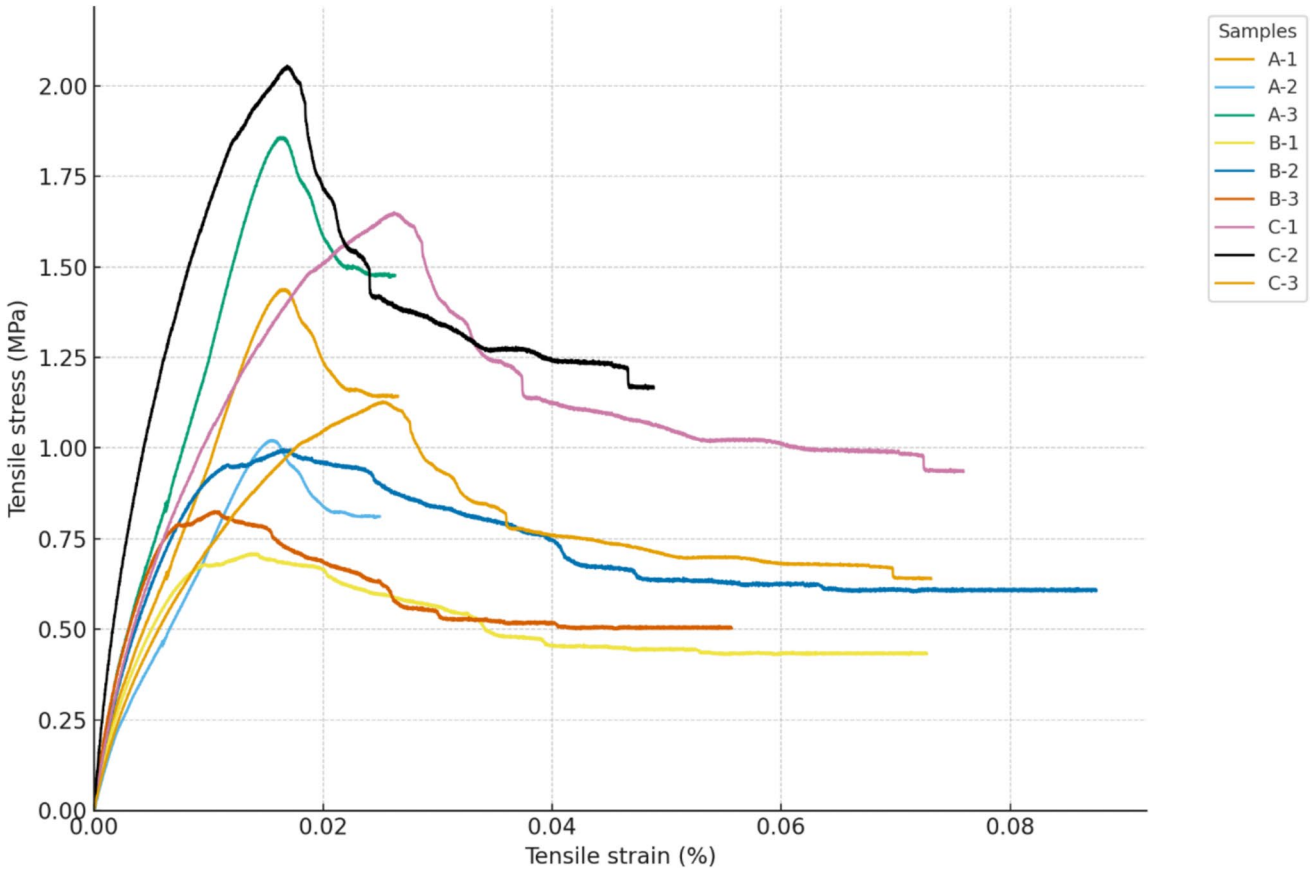

Fig. 10 Stress–strain graph for tensile strength

intercellular debonding and brittle fiber rupture, consistent with their higher peak stresses but reduced ductility. Comparable mechanism-based improvements have been demonstrated when the fiber/matrix interface is deliberately engineered. For example, in nettle fiber–reinforced epoxy, MgO nanoparticles enhanced load transfer, pinned/deflected cracks, and raised strength/stiffness by creating nano-scale bridges between fiber and matrix (Raja et al. 2024a). These findings suggest a practical route to mitigate the brittle tensile failure observed in our woody ring sections: combining CC fractions with surface modification (e.g., mild alkali/silane) and functional nano-fillers (MgO or similar) to toughen the matrix and improve interfacial shear.

Sample-level results (Table 6) show sample A displayed moderate tensile performance, averaging 1.44 MPa stress at ~ 2.4% strain, while sample B was notable for its ductility, sustaining strains above 7% but at lower stress levels (0.84 MPa). By contrast, Sample C combined higher stress values (1.64 MPa average) with intermediate strains (6.60%). These outcomes indicate that different radial fractions of the cob exhibit unique combinations of stiffness and ductility, governed by their tissue composition. The sectional differences observed here suggest functional specialization within corncob anatomy. The woody ring may be more suited for filler roles where tensile performance is less critical, the pith could serve in applications requiring ductility and energy absorption (e.g., acoustic or insulation panels), while the glume shows potential for reinforcement applications in particleboards or lightweight composites. This duality of ductility in pith and brittleness in woody fibers is characteristic of anisotropic plant-based materials.

The overall tensile modulus averaged 191.19 MPa (see Table 7), reflecting the stiffness of CC and its ability to resist deformation under stretching. This value corresponds to the integrity of the lignocellulosic matrix, where intermolecular bonding among cellulose, hemicellulose, and lignin provides resistance against fiber pull-out and slippage. The relatively low coefficient of variation (7.68%) for Young's modulus indicates consistent elastic behavior across different CC samples, suggesting uniform structural integrity at the molecular level. The maximum force analysis shows considerable variation with a coefficient of variation of 32.44%, reflecting the heterogeneous nature of the corncob structure and the differential load-bearing capacity of various sections. The middle section demonstrated the lowest maximum force capacity (0.0794 kN), while the lower and upper sections showed similar performance (0.1517 kN and 0.1497 kN, respectively). This pattern suggests that the middle section contains a higher proportion of softer pith material, while the extremities have greater concentrations of stronger woody components. Displacement analysis reveals the highest variability (coefficient of variation of 44.89%), indicating significant differences in deformation capacity across CC samples. This behavior is attributed to the characteristic of materials with high pith content, which can undergo substantial deformation before failure. The negative skewness values for all measured variables indicate a slight tendency toward higher values, suggesting that the majority of samples perform better than the mean, with fewer samples exhibiting poor performance. This distribution pattern is favorable for practical applications as it indicates consistent quality with occasional superior performance rather than frequent inferior results.

Previous research on similar agricultural residues provides valuable context for these findings. Wheat straw reported modulus values ranging from 130 to 333 MPa, depending on moisture content and processing conditions (Reddy & Yang 2005a), while tensile testing of barley straw yielded an average of 169 MPa (O'Dogherty et al. 1995). Among similar fibrous crop residues composed of cellulose, hemicellulose, and lignin, the CC's modulus of 191.19 MPa is comparable to that of sugarcane bagasse (186 MPa) and rice straw (211 MPa), as determined through experimental characterization (Teixeira et al. 2009; Sabeen et al. 2013). The corncob's tensile properties position it favorably among agricultural residues for construction applications. Its combination of moderate

Table 6 Tensile strength result

Sample	Sample ID	Max strain (%)	Max stress (MPa)
Sample A	A-1	2.65	1.44
	A-2	2.49	1.02
	A-3	2.63	1.86
	average	2.59 ± 0.07	1.44 ± 0.34
Sample B	B-1	7.27	0.71
	B-2	8.75	1.00
	B-3	5.56	0.83
	average	7.20 ± 1.30	0.84 ± 0.12
Sample C	C-1	7.59	1.65
	C-2	4.89	2.06
	C-3	7.31	1.13
	average	6.60 ± 1.21	1.61 ± 0.38

Table 7 Descriptive statistics of tensile strength

Variable	Sample A	Sample B	Sample C	Mean	StDev	CoefVar	Skewness
Young's modulus (MPa)	170.43	202.40	200.76	191.19	14.69	7.68	-0.70
Max force (kN)	0.15	0.07	0.15	0.12	0.03	26.48	-0.70
Displacement (mm)	2.08	7.65	5.7177	5.15	2.30	44.82	-0.35

strength (average maximum stress of 0.12 MPa) and good ductility (average displacement of 5.15 mm) provides a balanced performance profile suitable for applications requiring load-bearing capacity and energy absorption. For material application, it can serve as moisture-regulating materials for indoor environments, taking advantage of the material's hygroscopic nature. Additionally, the fibrous nature of CCs could be exploited in the production of fiberboards or particle boards for interior construction, providing alternatives to wood-based products and reducing pressure on forest resources (Ramos et al. 2021; Okeke et al. 2024c). Though previous studies demonstrated that the biomass ash can find useful application as Supplementary Cementitious materials in concrete production because of its alumina and silica content (Adesanya and Raheem 2010).

Fiber composition of corncob

The fiber composition of CC is a complex amalgamation of various components that contribute to its structural integrity and diverse applications. These fibers serve integral roles in plant anatomy, conferring support, flexibility, and functionality. Analysis revealed the following composition by weight: 42.5% ± 2.1% cellulose, 34.8% ± 1.7% hemicellulose, 18.3% ± 0.9% lignin, 1.0% ± 0.1% pectin, and 4.21% ± 0.21% resistant starch (mean ± SD), although published values demonstrate natural variability dependent on corn cultivar, maturity level, and processing methodology. The complex fiber matrix imparts the unique chemical and physical properties of CC advantageous for diverse material applications. The average lignocellulose composition of the corncob reported by several researchers is in the range of 33–43% cellulose, 26–36% hemicellulose, and 17–21% lignin (Qing et al. 2015; Bhatia et al. 2020). These data invariably show the high hemicellulose composition of corncob compared with other biomass types, such as wheat straw, rice straw, sugarcane bagasse, softwood, and kenaf, which typically range from 15% to 32% (Sarkar et al. 2012; Canilha et al. 2011; Ashori et al. 2011). Table 8 gives a detailed explanation of the fiber composition and various applications.

The mechanical properties of CC fibers are intricately governed by the contents of cellulose and lignin, serving as pivotal determinants in their fibrous structure. These fiber components exert diverse degrees of influence. Cellulose, characterized by stable linear polymer chains, plays a key role. The natural cellulose present in CC fibers exhibits a complicated consolidated structure, forming an extended molecular network. This intricate structure is further enveloped by external hemicellulose and lignin, resulting in the creation of a stronger and more cohesive composition. The strengthening effect of cellulose molecular chains of the microstructure activates on the application of external stress, thereby markedly boosting the mechanical strength of the corncob.

Lignin, a binding and filling agent in the skeleton of the fiber, significantly enhances structural strength and cell rigidity (Nandal et al. 2021). However, Zou et al. (2021) highlight that as the lignin content in the corncob increases, the microstructure becomes more tightly bound. However, this increase in lignin comes at the expense of cellulose reduction. Since cellulose contributes to the structural framework or skeleton of the CC, a decrease in cellulose content results in a weakened cellulose skeleton. Consequently, the reduction in the cellulose skeleton leads to a decrease in the overall mechanical strength of the CC. Hemicellulose, on the other hand, possesses a relatively low degree of polymerization and exhibits an unstable chemical structure and a limited degree of polymerization. Due to these characteristics, hemicellulose has a lesser impact on the mechanical properties of the CC compared to cellulose and lignin. Therefore, the relationship between hemicellulose concentration and mechanical characteristics is regarded as non-significant.

Practical applications of Corncob as Sustainable Building Material

Based on the comprehensive characterization of CC morphology, mechanical properties, and chemical composition, multiple potential applications in sustainable construction have been identified.

- **Load-sharing cores, skins, and lightweight structural elements**
- The upper and middle cob sections, which are woody ring–rich, recorded the highest compressive capacities (upper: 115.72 ± 6.49 MPa; middle: 65.82 ± 14.80 MPa), whereas the lower (pith-rich) section was weakest (21.26 ± 2.11 MPa). This stratification indicates that fractionating CC and prioritizing upper/middle fractions as fillers or laminates can deliver reliable compressive load-sharing in sandwich skins, ribbed panels, and webs of secondary beams. The section-resolved failure mode (radial cracking initiating from the pith and arrested by the woody ring) supports using woody-rich fractions where crack containment is desirable. Average compressive performance across all sections (67.6 MPa) further positions CC among competitive natural biomaterials for non-critical load paths where mass-specific properties matter. Microstructurally, SEM shows dense, layered fibrous networks in the woody ring that underpin stiffness, while glume/pith porosity explains the observed buffering at low strains; this validates a materials-by-design approach in which woody fractions serve in stiff cores/skins and pith fractions provide local energy dissipation.

Table 8 Fiber composition of CC and application

Description			Refs
Cellulose	Cellulose is the most abundant natural linear polymer of glucose and a major component of the plant cell wall. CC contain a significant amount of cellulose, contributing to their structural integrity		Ali et al., (2020)
	Properties	Cellulose fibers are known for their high tensile strength and rigidity, and resistance to enzymatic degradation. Degree of Polymerization (DP) is 600–1000. Crystallinity index is 43–48% and it is mostly microfibrils with diameter 10–30 nm	
	Uses	Cellulose extracted from CC can be used in the production of biofuels, textiles, insulation, and paper	
Building material applications		Reinforcement in bio-composites for improved mechanical properties	
		Production of nanocellulose for high-performance building materials	
		Binder in particleboards and fiberboards	
Hemicellulose	Hemicellulose is a branched polymer that surrounds cellulose microfibrils in the plant cell wall. CCs have a notable hemicellulose content, influencing their overall composition.		Oshido et al., (2024)
	Properties	Hemicellulose fibers are more flexible than cellulose, providing elasticity to plant cell walls and exhibit different chemical properties than cellulose. Main types include arabinoxylans and glucomannans with lower DP compared to cellulose (50-300).	
	Uses	Hemicellulose can be used in the production of adhesives, coatings, and as a component in animal feed	
Building material applications		Natural binding agent in particleboard production	
		Contributes to water absorption properties in insulation materials	
Lignin	Lignin is a complex, non-carbohydrate aromatic polymer that provides rigidity to plant cell walls. CC contain lignin, especially in the outer layers		Pointner et al., (2014)
	Properties	Lignin enhances the resistance of plant fibers to decay and microbial attack because it can be challenging to break down. Mostly guaiacyl (G) and syringyl (S) units with complex 3D structure	
	Uses	Lignin extracted from corncobs has applications in the production of bio-based materials, such as bioplastics	
Building material applications		Natural adhesive in eco-friendly building panels	
		Flame retardant additive in insulation materials	
		Precursor for carbon fibers in high-strength composites	

Table 8 (continued)

Description		Refs
Pectin	Pectin is a complex polysaccharide found in the middle lamella of plant cells. Although not as abundant as in some fruits, corncobs do contain pectin.	Zhang et al., (2015)
	Properties	
	Pectin contributes to the viscosity and gelling properties of plant tissues. Mainly galacturonic acid	
	Uses	
	Pectin extracted from corncobs can find applications in the food industry as a gelling agent in jams and jellies	
Building material applications		
	Improves water resistance in corncob-based insulation materials	
	Enhances bonding in particleboard production	
Resistant starch	Resistant starch is a type of starch that resists digestion in the small intestine. CCs contain starch, with some proportion being resistant starch	
	Properties	
	Resistant starch has potential health benefits, acting as a prebiotic promoting the growth of beneficial gut bacteria. Mainly type 2 resistant starch	
	Uses	
	Resistant starch from corncobs has potential applications in functional foods with health benefits and adhesive production	
	Biodegradable binder in eco-friendly construction materials	
Building material applications		
	Enhances moisture buffering capacity in indoor applications	

- **Lightweight concrete and bio-aggregate blocks**
- The balanced strength–ductility profile (high section-dependent compressive stress with progressive yielding) makes CC a candidate lightweight bio-aggregate for non-load-bearing blocks, infill panels, and stay-in-place form units. The upper/middle fractions (woody-dominant) can boost early age bearing and reduce creep-like deformation under service compression, while the pith fraction's cellular porosity helps lower density and improve toughness against impact or handling damage.
- **Structural boards and particle/fiber-based panels**
- The tensile characterization returned an overall Young's modulus of 191.19 MPa with modest dispersion (Coef-Var ≈ 7.68%), indicating a consistent elastic response at small strains useful for panel products that rely on elastic recovery (e.g., subflooring underlay and interior sheathing). Samples exhibited a trade-off between strength and ductility, suggesting that blending woody ring and glume-rich fines can tune stiffness vs. toughness in boards. The rough, high-area surfaces observed in SEM (glume/woody ring) support good mechanical interlocking with bio-binders, while lignin's native adhesiveness can reduce synthetic resin demand.
- **Thermal–acoustic insulation systems**
- Pith and glume exhibit pronounced cellular porosity (honeycomb-like voids and sheeted layers), which explains the initial compressive buffering seen in the stress–strain curves and can directly support thermal and acoustic attenuation (Bovo et al. (2022). Leveraging these layers as the dominant fraction in mats, baffles, or composite "quiet wall" facings should reduce heat transfer and absorb mid–high-frequency sound; SEM evidence of interconnected pores indicates combined absorption and damping mechanisms.
- **Hygrothermal buffering and moisture-active liners**
- The pith's open, interconnected structure, coupled with the ductile tensile response of pith-rich specimens, points to moisture buffering liners or ceiling panels that accommodate cyclic swelling/shrinkage without brittle failure. The measured elastic modulus with low variance suggests predictable small-strain behavior during daily humidity cycling.
- **Cementitious hybrids and SCM adjacent roles**
- EDS mapping shows elevated Si (2.52 wt%) and Al (0.69 wt%) in the glume, compared to trace levels in the pith, consistent with mineral-like behavior and potential reactivity pathways when thermally processed e.g., ash or pozzolanic blends (Okeke et al. 2024a). This supports using glume-enriched fines/ash as a supplementary phase in cementitious composites, while woody ring/pith fractions act as lightweight fillers to tailor density and crack-bridging.
- **3D-printable bio-composites and molded skins**

- The combination of (i) steady small-strain stiffness (E ≈ 191 MPa), (ii) section tailorable ductility, and (iii) rough, fibrous surfaces (SEM) that enhance matrix adhesion, enables CC-filled biopolymers for large-bead additive manufacturing (e.g., stay-in-place formwork shells, ribbed facade modules). Here, woody ring fibers contribute stiffness and dimensional stability; pith/glume add damping and weight reduction. Also, CC-based polymers can be integrated into 3D printing filaments, creating customizable and sustainable building components (Hassan et al. 2024).
- **Carbon-storing interior products and stay-in-place formwork**
- High carbon content across all tissues (≈ 64–68 wt% C; ≈ 31–34 wt% O) underpins the role of CC-based products as carbon stores in long-lived interior applications (wall linings, trims, and acoustic tiles). In stay-in-place formwork, CC panels add thermal resistance and mass-specific rigidity while retaining the biogenic carbon in the fabric of the building.

Preliminary life cycle assessment (LCA) phases

Raw material acquisition Corncob (CC) is an agricultural by-product; using it diverts a waste stream at near-zero feedstock cost. Our EDS results show high biogenic carbon (64–68 wt% C), meaning CC enters the system already storing carbon rather than requiring carbon-intensive extraction. Because collection typically occurs close to farms and settlements, transport distances and masses are modest; coupled with CC's low density (supported by the porous pith/glume seen in SEM), this lowers transport energy and CO_2e per kilogram relative to mineral aggregates. In practice, smallholder collection and short-haul transport can yield order-of-magnitude reductions compared with quarry-to-plant logistics; our working assumption is a ~ 0.05–0.10 kg CO_2e cut per kg delivered where local sourcing is feasible.

Processing CC's conversion into building intermediates (cleaning, grading, drying, and size reduction) is mechanically simple and typically low temperature. The main energy hotspots are drying and milling; both are amenable to optimization (air/solar drying, right-sizing particle geometry to the target matrix). When thermally processed to ash for supplementary cementitious material (SCM), published factors indicate 0.002 kg CO_2/kg and 0.022 MJ/kg, versus Portland cement at 0.82 kg CO_2/kg and 5.50 MJ/kg—i.e., ~ 99.7% lower embodied carbon and ~ 99.6% lower embodied energy per kilogram of binder replaced (Bheel and Adesina 2021). The EDS-mapped Si/Al enrichment in the glume fraction further supports selective upgrading of glume-rich fines to reactive ash, while woody/pith fractions feed low-energy bio-aggregate streams.

Use phase (application) The microstructures observed in SEM (cellular pith and fibrous woody ring) explain the dual performance measured: robust compressive response (upper/middle sections strongest) and small-strain tensile stiffness (E ≈ 191 MPa) with controlled ductility. These traits translate into durable, lightweight panels, infills, and composites that resist handling damage and accommodate service deformations, potentially extending service life and reducing replacement cycles (a key driver of life cycle impacts). The same porosity that lowers density also underpins thermal and acoustic attenuation reported for CC-based products (Sidharta et al. 2022); in composite skins/cores it can reduce operational energy demand when used as insulation or thermal breaks. Low-VOC binder options align with CC's lignocellulosic chemistry, limiting indoor air-quality burdens.

End-of-life CC rich products are intrinsically biodegradable/compostable when not immobilized in high cement matrices. Where separation is feasible, clean fractions can be composted, used as biomass fuel, or calcined to SCM ash, closing loops and displacing virgin clinker. Two practical constraints may be noted: (i) design for disassembly to separate CC from polymeric or cementitious matrices, and (ii) local infrastructure for composting or ash valorization. Both can be addressed through product design (mechanical fastening, reversible binders) and regional partnerships with agriculture and cement plants. Although areas for further studies and development.

Potential environmental impact

Carbon footprint reduction CC stores biogenic carbon (confirmed by EDS), and the mechanical results justify its substitution into real components (not merely fillers), increasing the mass of carbon retained in long-lived products. On the manufacturing side, minimal processing and low transport intensities lower cradle-to-gate emissions. Where CC ash substitutes part of Portland cement, the cited factors imply ~ 99% lower embodied carbon per kilogram of binder replaced. In the use phase, CC-based insulation and lightweight composites can curb operational energy, compounding embodied savings. Altogether, CC enables carbon reduction across all stages: stored carbon in the product, low-carbon processing, and demand-side energy savings.

Resource conservation Valorizing CC displaces virgin mineral extraction (aggregates, some binders) and reduces pressure on timber resources for certain board/insulation applications. The section-resolved strength and stiffness allow targeted use of woody ring-rich fractions where mechanical performance is needed and pith/glume where functional porosity is prized—delivering "material where it matters"

and avoiding over-specification. Water and temperature demands in processing are modest compared with ceramics or clinker; adopting ambient/solar drying strategies can further reduce blue-water and energy use.

Waste management and circularity CC utilization converts an often-burned or landfilled residue into economic value, avoiding open-field burning emissions and methane from anaerobic decay. The findings on Si/Al localization in glume and the demonstrated structural contribution of woody fractions suggest two credible end-of-life routes: (i) clean, separated CC back to soil or bioenergy; (ii) contaminated fractions to controlled calcination for SCM, closing a technical loop with the cement sector. Designing products for separability (releasable fasteners, dissolvable or bio-based binders) will unlock cradle-to-cradle pathways at scale.

Revenue generation Transforming corncobs into building materials also creates economic value from waste products, supporting circular economy principles. This valorization of agricultural waste not only contributes to environmental sustainability but also provides a viable income source for farmers, encouraging greater adoption of sustainable practices across the agricultural sector. By promoting the use of corncob-based materials, the construction industry becomes an active participant in reducing waste and enhancing resource efficiency.

Conclusion

The CC represents an underutilized yet promising biomaterial resource demonstrating unique structural and compositional attributes translatable to diverse building and sustainability applications. Fundamental insights uncovered through systematic multi-scale examination of morphology, mechanical performance, and chemical constituents establish a foundation for optimizing CC waste valorization. The compression testing showed a clear strength hierarchy (upper $\gg$ middle $\gg$ lower): the woody ring–rich upper section averaged ~ 115.7 MPa, the middle ~ 65.8 MPa, and the pith-dominated lower ~ 21.3 MPa, with an overall mean $\approx$67.6 MPa competitive among natural biomaterials for non-critical load paths. These values track directly with the observed microstructure: dense, fibrous woody rings conferring stiffness and crack arrest, versus porous pith and glume providing energy dissipation and low density. Under tension, CC exhibited a consistent small-strain stiffness (Young's modulus = 191.2 MPa; low dispersion), with section-dependent trade-offs between strength and ductility. This anisotropic response aligns with the SEM evidence of laminated cell wall architectures and interfacial sliding mechanisms that accommodate deformation without catastrophic failure. Together, these results justify fractionation: woody-rich fractions for load-sharing cores/skins and pith/glume for lightweight, damping, and insulation roles. Chemically, EDS confirmed high biogenic carbon across tissues (64.7–67.7 wt% C; 31–34 wt% O), underpinning carbon storage in long-lived products. Critically, the glume concentrates mineral surrogates (Si $\approx$2.52 wt%, Al $\approx$0.69 wt%), supporting pathways to reactive ashes or SCM adjacent hybrids, while woody/pith fractions remain ideal as bio-aggregates. These composition–structure links explain the measured mechanics and open low-energy processing routes. A preliminary LCA framing indicates potential cradle-to-gate advantages driven by low-mass collection, minimal processing, and partial cement displacement via CC ash; at end-of-life, CC's biodegradability and ash valorization enable circular options where separation is designed in. While indicative, these gains require system-bound validation at scale.

The study contributes (i) a tissue-level map connecting CC morphology and chemistry to tensile/compressive response, (ii) a clear materials-by-design strategy via anatomical fractionation, and (iii) early life cycle reasoning to guide productization. CC is therefore a credible, locally available feedstock for insulation, sandwich cores/skins, particle/fiber boards, and cementitious hybrids, provided products are engineered for moisture, durability, and circularity constraints identified here. Its elemental findings cement the potential for composite formulations of processed cob fibers to displace conventional materials in various building, insulation, 3D printing, and load-bearing applications. Specifically, the balanced ductility and durability performance recorded, coupled with low ecosystem impacts, position this annually renewable biomass as an auspicious sustainable substitute for mainstream construction and temperature control usages.

Further areas of study

Though the present study provided insight into Composition-Structure–Function relations in CC fibers, additional inquiries should concentrate on comprehensive LCA and techno-economics replacing preliminary assumptions with measured logistics, interface engineering for tensile toughness and durability mechanics under real climates quantifying long-term creep, fatigue, and fracture for woody-rich vs. pith-rich fractions under coupled humidity–temperature cycling, linking failure modes to the SEM-resolved architectures that governed strength here.

Acknowledgements Authors wish to appreciate the technical assistance of both the engineering workshop and life sciences laboratory technicians of Canterbury Christ Church University for their support in this research.

Author contributions Francis Okeke contributed to conceptualization, data collection, method, analysis, writing—original draft, discussion, and final editing. Abdullahi Ahmed contributed to method, analysis, and editing. Adil Imam contributed to literature review, validation of results and method. Hany Hassanin contributed to method, discussion, analysis, and final editing.

Funding This research did not have the courtesy of any funding from any organization.

Data availability The authors confirm that the data supporting the findings of this study are available within the article.

Declarations

Competing interests The authors declare that they have no known competing financial interests or personal relationships that could have appeared to influence the work reported in this paper.

Consent to publish All named authors in the paper have agreed that the manuscript be submitted for publication.

Ethical approval The study adhered to the ethics guidelines of the Canterbury Christ Church University and followed the Declaration of Helsinki—principles of informed consent, voluntary participation and withdrawal, confidentiality, and privacy of the participants.

References

Adesanya DA, Raheem AA (2010) A study of the permeability and acid attack of corn cob ash blended cements. Constr Build Mater 24(3):403–409

Ali JB, Danladi A, Bukhari MM, Nyakuma BB, Mamza P, Mohamad ZB, Musa AB, Inuwa IM (2020) Extraction and characterization of cellulose nanofibres and cellulose nanocrystals from Sammaz-14 maize cobs. J Nat Fibers 19(7):2756–2771. https://doi.org/10.1080/15440478.2020.1856279

Andrew JJ, Dhakal HN (2022) Sustainable biobased composites for advanced applications: recent trends and future opportunities – a critical review. Composites Part C: Open Access 7:100220. https://doi.org/10.1016/j.jcomc.2021.100220

Aschemann-Witzel J, de Hooge I, Amani P, Bech-Larsen T, Oostindjer M (2015) Consumer-related food waste: causes and potential for action. Sustainability 7(6):6457–6477. https://doi.org/10.3390/su7066457

Ashori A, Hamzeh Y, Amani F (2011) Lemon balm (*Melissa officinalis*) stalk: chemical composition and fiber morphology. J Environ Polym Degrad 19(1):297–300. https://doi.org/10.1007/s10924-010-0279-8

Bhatia SK, Jagtap SS, Bedekar AA, Bhatia RK, Patel AK, Pant D, Yang YH (2020) Recent developments in pretreatment technologies on lignocellulosic biomass: effect of key parameters, technological improvements, and challenges. Bioresour Technol 300:122724

Bheel N, Adesina A (2021) Influence of binary blend of corn cob ash and glass powder as partial replacement of cement in concrete. SILICON 13:1647–1654. https://doi.org/10.1007/s12633-020-00557-4

Blanco-Canqui H, Lal R (2007) Soil and crop response to harvesting corn residues for biofuel production. Geoderma 141(3–4):355–362. https://doi.org/10.1016/j.geoderma.2007.06.012

Bonin C, Lal R (2012) Agronomic and ecological implications of biofuels production on soil processes: carbon and nitrogen cycles, soil biodiversity, and ecosystem services. In: Tomes D, Lakshmanan P, Songstad D (eds) Biofuels: global impact on renewable energy, production agriculture and technological advancements. Springer, Berlin

Bovo M, Giani N, Barbaresi A, Mazzocchetti L, Barbaresi L, Giorgini L, Tassinari P (2022) Contribution to thermal and acoustic characterization of corn cob for bio-based building insulation applications. Energy Build 262:111994. https://doi.org/10.1016/j.enbuild.2022.111994

Brassard P, Godbout S, Raghavan V (2016) Pyrolysis in augmented facilities: a new potential approach for agricultural waste management in Québec (Canada). Environ Prog Sustain Energy 35(6):1627–1634. https://doi.org/10.1002/ep.12563

Canilha L, Chandel AK, Milessi TSS, Antunes FAF, Freitas WLC (2011) Bioconversion of sugarcane biomass into ethanol: an overview about composition, pretreatment methods, detoxification of hydrolysates, enzymatic saccharification, and ethanol fermentation. J Biomed Biotechnol. https://doi.org/10.1155/2012/989572

Castorina G, Cappa C, Negrini N et al (2023) Characterization and nutritional valorization of agricultural waste corncobs from Italian maize landraces through the growth of medicinal mushrooms. Sci Rep 13:21148. https://doi.org/10.1038/s41598-023-48252-9

de Hooge IE, Oostindjer M, Aschemann-Witzel J, Normann A, Loose SM, Almli VL (2017) This apple is too ugly for me!: consumer preferences for suboptimal food products in the supermarket and at home. Food Qual Prefer 56:80–92. https://doi.org/10.1016/j.foodqual.2016.09.012

Espinach FX, Julian F, Alcalà M, Vilaseca F, Carrasco F, Mutjé P (2022) Effective tensile strength estimation of natural fibers through micromechanical models: the case of henequen fiber reinforced-PP composites. Polymers 14(22):4890. https://doi.org/10.3390/polym14224890

Food and Agriculture Organization. (2023). Food and Agriculture Organization of the United Nations annual corn production. https://www.fao.org/faostat/en/#data/QCL/visualize

Gallagher, P. W., Dikeman, M., Fritz, J., Wailes, E., Gauthier, W., & Shapouri, H. (2003). Biomass from crop residues: cost and supply estimates (Agricultural Economic Report No. 819). United States Department of Agriculture. https://www.usda.gov/oce/reports/energy/AER819.pdf

Goel G (2021) A review on biomass-derived materials and their applications as corrosion inhibitors, catalysts, food and drug delivery agents. Current Res Green Sustain Chem. https://doi.org/10.1016/j.crgsc.2021.100153

Grunert KG, Hieke S, Wills J (2014) Sustainability labels on food products: consumer motivation, understanding and use. Food Policy 44:177–189. https://doi.org/10.1016/j.foodpol.2013.12.001

Gustavsson, J., Cederberg, C., Sonesson, U., Van Otterdijk, R., & Meybeck, A. (2011). Global food losses and food waste. Food and Agriculture Organization of the United Nations. http://www.fao.org/docrep/014/mb060e/mb060e.pdf

Hassan M, Mohanty AK, Misra M (2024) 3D printing in upcycling plastic and biomass waste to sustainable polymer blends and

composites: a review. Mater des 237:112558. https://doi.org/10.1016/j.matdes.2023.112558
Horwitz, W., & Latimer, G. W. (2005). Official methods of analysis of AOAC International (18th ed.). AOAC International.
Htsfarms (2022). White Maize variety. Available online @https://htsfarms.ng/product/maize-variety-sammaz-16-1kg/ (Accessed Jan 8th, 2023)
Jebadurai SG, Edwin Raj R, Sreenivasan VS, Binoj JS (2019) Comprehensive characterization of natural cellulosic fiber from *Coccinia grandis* stem. Carbohydr Polym 207:675–683. https://doi.org/10.1016/j.carbpol.2018.12.027
Johnson JM, Allmaras RR, Reicosky DC (2006) Estimating source carbon from crop residues, roots and rhizodeposits using the National grain-yield database. Agron J 98(3):622–636. https://doi.org/10.2134/agronj2005.0179
Kabir MM, Wang H, Lau KT, Cardona F (2013) Effects of chemical treatments on hemp fibre structure. Appl Surf Sci 276:13–23. https://doi.org/10.1016/j.apsusc.2013.03.023
Kaw AK (2005) Mechanics of composite materials, 2nd edn. CRC Press, Boca Raton
Kim S, Dale BE (2004) Global potential bioethanol production from wasted crops and crop residues. Biomass Bioenergy 26(4):361–375. https://doi.org/10.1016/j.biombioe.2003.08.002
Kummu M, de Moel H, Porkka M, Siebert S, Varis O, Ward PJ (2012) Lost food wasted resources: global food supply chain losses and their impacts on freshwater, cropland, and fertiliser use. Sci Total Environ 438:477–489. https://doi.org/10.1016/j.scitotenv.2012.08.092
Mayernik, J. (2020). Buildings energy data book. Office of Energy Efficiency & Renewable Energy, United States. https://data.openei.org/submissions/144
Nafziger, E. D. (2003). Corn planting. Illinois Agronomy Handbook, 24, 31-38
Nandal P, Arora A, Virmani S (2021) An appraisal on valorization of lignin: a byproduct from biorefineries and paper industries. Biomass Bioenergy 155:106295. https://doi.org/10.1016/j.biombioe.2021.106295
Neumann, C., & Bassler, R. (1976). VDLUFA methodenbuch band III die chemische untersuchung von futtermitteln 3. Darmstadt.
O'Dogherty MJ, Huber JA, Dyson J, Marshall CJ (1995) A study of the physical and mechanical properties of wheat straw. J Agric Eng Res 62(2):133–142. https://doi.org/10.1006/jaer.1995.1061
Okeke FO, Eziyi IO, Udeh CA, Ezema EC (2020) City as habitat: assembling the fragile city. Civ Eng J 6(6):1143–1154. https://doi.org/10.28991/cej-2020-03091536
Okeke FO, Ahmed A, Imam A, Hassanin H (2024a) A review of corncob-based building materials as a sustainable solution for the building and construction industry. Hybrid Adv. https://doi.org/10.1016/j.hybadv.2024.100269
Okeke FO, Ahmed A, Imam A, Hassanin H (2024b) Assessment of compressive strength performance of corn cob ash blended concrete: a review. In Sixth international conference on sustainable construction materials and technologies (Vol. 1). 606. https://doi.org/10.18552/2024/SCMT/606
Okeke FO, Ahmed A, Imam A, Hassanin H (2024c) Study on agricultural waste utilization in sustainable particleboard production. E3S web of conferences, 563, 02007. https://doi.org/10.1051/e3sconf/202456302007
Oshido BA, Ubwa ST, Oshido LE, Aondoaver SA, Adah CA (2024) Isolation and characterization of nanocellulose from corncobs. IOSR J Appl Chem 17(8):21–25
Penn S (2006) Penn state researchers use corn waste to generate electricity. Fuel Cells Bull 9:4–5. https://doi.org/10.1016/s1464-2859(06)71301-3
Pinto J, Cruz D, Paiva A, Pereira S, Tavares P, Fernandes L, Varum H (2012) Characterization of corn cob as a possible raw building material. Constr Build Mater 34:28–33. https://doi.org/10.1016/j.conbuildmat.2012.02.014
Pointner M, Kuttner P, Obrlik T, Jäger A, Kahr H (2014) Composition of corncobs as a substrate for fermentation of biofuels. Agron Res 12(2):391–396
Qing Q, Huang M, He Y, Wang L, Zhang Y (2015) Dilute oxalic acid pretreatment for high total sugar recovery in pretreatment and subsequent enzymatic hydrolysis. Appl Biochem Biotechnol 177:1493–1507
Raja T, Devarajan Y, Logesh K, Rajiv A, Upadhye VJ, Tiwari K (2024a) An in-depth investigation into the utilization of nettle fiber-reinforced epoxy composites with embedded MgO nanoparticles. J Reinf Plast Compos. https://doi.org/10.1177/07316844241266650
Raja T et al (2024b) Study on the characteristics of novel fiber extracted from Foxtail palm fruits—a steps towards the sustainable development. Mater Lett 373:137145. https://doi.org/10.1016/j.matlet.2024.137145
Ramos A, Briga-Sá A, Pereira S, Correia M, Pinto J, Bentes I, Teixeira CA (2021) Thermal performance and life cycle assessment of corn cob particleboards. J Build Eng 44:102998
Reddy N, Yang Y (2005a) Biofibers from agricultural byproducts for industrial applications. Trends Biotechnol 23(1):22–27
Reddy N, Yang Y (2005b) Structure and properties of high quality natural cellulose fibers from corn stalks. Polymer 50(15):47–53. https://doi.org/10.1016/j.polymer.2009.05.017
Sabeen M, Ngadi M, Raghavan GSV, Kenney I (2013) Rheological characterization of raw and enzymatically hydrolyzed sweet sorghum bagasse. Ind Crops Prod 43:647–653. https://doi.org/10.1016/j.indcrop.2012.08.014
Sagar NA, Pareek S, Sharma S, Yahia EM, Lobo C (2018) Fruit and vegetable waste: bioactive compounds, their extraction, and possible utilization. Compr Rev Food Sci Food Saf 17(3):512–531. https://doi.org/10.1111/1541-4337.12330
Sarkar N, Ghosh SK, Bannerjee S, Aikat K (2012) Bioethanol production from agricultural wastes: an overview. Renew Energy 37(1):19–27. https://doi.org/10.1016/j.renene.2011.06.045
Serra-Parareda F, Vilaseca F, Aguado R, Espinach FX, Tarrés Q, Delgado-Aguilar M (2021) Effective Young's modulus estimation of natural fibers through micromechanical models: the case of Henequen fibers reinforced-PP composites. Polymers 13(22):3947. https://doi.org/10.3390/polym13223947
Setter TL, Flannigan BA, Melkonian J (2001) Loss of kernel set due to water deficit and shade in maize: carbohydrate supplies, abscisic acid, and cytokinins. Crop Sci 41(5):1530–1540. https://doi.org/10.2135/cropsci2001.4151530x
Sidharta M, Sudarsono AS, Hariyanto AD, Arifin LS (2022) Corn cob absorption rate as acoustic material. J Appl Sci, Eng, Technol, Education 4(1):88–96. https://doi.org/10.35877/454RI.asci984
Sun X-F, Sun R-C, Su Y, Sun J-X (2004) Comparative study of crude and purified cellulose from wheat straw. J Agric Food Chem 52(4):839–847. https://doi.org/10.1021/jf0349230
Takada M, Niu R, Minami E, Saka S (2018) Characterization of three tissue fractions in corn (*Zea mays*) cob. Biomass Bioenergy 115:130–135. https://doi.org/10.1016/j.biombioe.2018.04.023
Tao T, Wei X (2020) Analysis of impact characteristics of corn cob based on LSDYNA. J Agricultural Mech Res 42:27–31, 145
Teixeira EM, Pasquini D, Curvelo AAS, Corradini E, Belgacem NM, Dufresne A (2009) Cassava bagasse cellulose nanofibrils reinforced thermoplastic cassava starch. Carbohydr Polym 78:422–431. https://doi.org/10.1016/j.carbpol.2009.04.034
Thandavamoorthy R, Devarajan Y (2024) Study on the characteristics of Napier grass fibre reinforced porcelain filler particulates poly lactic acid matrix biocomposite. J Reinf Plast Compos. https://doi.org/10.1177/07316844241253912

U.S. Environmental Protection Agency, Office of Research and Development. (2021). From farm to kitchen: The environmental impacts of U.S. food waste (EPA 600-R-21–171). Authors: Kirsten Jaglo, Shannon Kenny, & Jenny Stephenson. https://doi.org/10.23719/1526935

U.S. Department of Agriculture, Foreign Agricultural Service. (2025). World agricultural production report. United States Department of Agriculture. Available on @ Corn | USDA Foreign Agricultural Service accessed 12/08/2025

Uribelarrea M, Below FE, Moose SP (2004) Grain composition and productivity of maize hybrids derived from the Illinois protein strains in response to variable nitrogen supply. Crop Sci 44(5):1593–1600. https://doi.org/10.2135/cropsci2004.1593

Van Soest PJ, Robertson JB, Lewis BA (1991) Methods for dietary fiber, neutral detergent fiber, and nonstarch polysaccharides in relation to animal nutrition. J Dairy Sci 74(10):3583–3597. https://doi.org/10.3168/jds.S0022-0302(91)78551-2

Wojcieszak D, Przybył J, Czajkowski Ł, Majka J, Pawłowski A (2022) Effects of harvest maturity on the chemical and energetic properties of corn stover biomass combustion. Materials 15(8):2831. https://doi.org/10.3390/ma15082831

Yan, H.L. (2017) Study on mechanical properties and in-situ characteristics of maize. Master's Thesis, Jilin University, Changchun, China,

Yanni SF, Whalen JK, Ma BL (2013) Corn cobs as a potential source of fuel ethanol production and soil amendment. American J Energy Res 1:13–22

Yu, J. (2014). Measurement and analysis of the physical and mechanical properties of corn ears [Doctoral dissertation]. JiLin University.

Zhang Y, Ding L, Gu J, Tan H, Zhu L (2015) Preparation and properties of a starch-based wood adhesive with high bonding strength and water resistance. Carbohydr Polym 115:32–37. https://doi.org/10.1016/j.carbpol.2014.08.063

Zou Y, Fu J, Chen Z, Ren L (2021) The effect of microstructure on mechanical properties of corn cob. Micron 146:103070